

Advances in Vascular Diagnostics using Magnetic Particle Imaging (MPI) for Blood Circulation Assessment

Marisa O Pacheco, Isabelle K Gerzenshtein, Whitney L Stoppel, and Carlos M Rinaldi-Ramos*

Rapid and accurate assessment of conditions characterized by altered blood flow, cardiac blood pooling, or internal bleeding is crucial for diagnosing and treating various clinical conditions. While widely used imaging modalities such as magnetic resonance imaging (MRI), computed tomography (CT), and ultrasound offer unique diagnostic advantages, they fall short for specific indications due to limited penetration depth and prolonged acquisition times. Magnetic particle imaging (MPI), an emerging tracer-based technique, holds promise for blood circulation assessments, potentially overcoming existing limitations with reduction in background signals and high temporal and spatial resolution, below the millimeter scale. Successful imaging of blood pooling and impaired flow necessitates tracers with diverse circulation half-lives optimized for MPI signal generation. Recent MPI tracers show potential in imaging cardiovascular complications, vascular perforations, ischemia, and stroke. The impressive temporal resolution and penetration depth also position MPI as an excellent modality for real-time vessel perfusion imaging via functional MPI (fMPI). This review summarizes advancements in optimized MPI tracers for imaging blood circulation and analyzes the current state of pre-clinical applications. This work discusses perspectives on standardization required to transition MPI from a research endeavor to clinical implementation and explore additional clinical indications that may benefit from the unique capabilities of MPI.

1. Introduction

From coronary heart disease, to stroke, to internal vascular trauma, diagnostic imaging is required across many clinical indications. Specifically, imaging the movement of red blood cells

M. O Pacheco, W. L Stoppel, C. M Rinaldi-Ramos Chemical Engineering University of Florida Gainesville, FL 32611, USA E-mail: carlos.rinaldi@ufl.edu

I. K Gerzenshtein Microbiology and Cell Science University of Florida Gainesville, FL 32611, USA

W. L Stoppel, C. M Rinaldi-Ramos J. Crayton Pruitt Family Department of Biomedical Engineering University of Florida

Gainesville, FL 32611, USA

The ORCID identification number(s) for the author(s) of this article can be found under https://doi.org/10.1002/adhm.202400612

DOI: 10.1002/adhm.202400612

Adv. Healthcare Mater. 2024, 2400612

in the body is critical for the diagnosis and detection of many diseases and injuries, as well as the assessment of brain function. Thus, the past several decades has seen substantial growth in the application and modification of existing imaging techniques and the investigation of new methods to address current diagnostic needs. In this review, we will explore the development, characterization, and standardization of an emerging imaging modality, magnetic particle imaging (MPI),[1-3] specifically for applications in tracking blood flow, perfusion, and injury. To understand the gaps in existing technologies that have motivated the investigation of MPI for tracking blood pooling in the heart and systemic blood flow, we will first briefly review current techniques and clinical practices, highlighting limitations of current techniques and areas for improvement.

1.1. Angiography for Diagnosis and Treatment of Vascular Disease

Angiography, defined as the visualization of the circulatory system, is an important diagnostic technique used to identify treatments

for a myriad of diseases and injuries. Clinically, angiography is used to evaluate cardiac function, delineate vessels, detect internal bleeding, and to assess organ perfusion and ischemia.^[4] The circulatory system is involved across all organ systems and is affected by the onset and progression of the most prevalent diseases, including cardiac disease and cancer.^[5] Improved diagnostic tools can enable the safe and early detection of disturbances to circulatory function.^[6] Early detection is often correlated with improved outcomes, indicating the need for investment in the development of diagnostic imaging tools and techniques for early detection. There are two main techniques that are often coupled together to evaluate and diagnose patients: 1) analysis of vessel structures and cardiac function using catheterization; and 2) non-invasive imaging of blood vessels for the visualization of perfusion, hemorrhage, and blood pooling (Figure 1).

The earliest clinical tools for mapping circulation emerged in the 1920s with catheter-based techniques.^[10] These techniques involve the insertion of a catheter into large vessels in the groin or arm enabling both diagnosis and intervention. Cardiac catheterization, commonly known as a "heart cath" procedure, has

2192559, 0, Downloaded from https://onlinelibrary.wiley.com/doi/10.1002adm.202400612 by University Of Florida, Wiley Online Library on [01/07/2024]. See the Terms and Conditions (https://onlinelibrary.wiley.com/terms-and-conditions) on Wiley Online Library for rules of use; OA articles are governed by the applicable Creative Commons Licensean Conditions (https://onlinelibrary.wiley.com/terms-and-conditions) on Wiley Online Library for rules of use; OA articles are governed by the applicable Creative Commons Licensean Conditions (https://onlinelibrary.wiley.com/terms-and-conditions) on Wiley Online Library for rules of use; OA articles are governed by the applicable Creative Commons Licensean Conditions (https://onlinelibrary.wiley.com/terms-and-conditions) on Wiley Online Library for rules of use; OA articles are governed by the applicable Creative Commons Licensean Conditions (https://onlinelibrary.wiley.com/terms-and-conditions) on Wiley Online Library for rules of use; OA articles are governed by the applicable Creative Commons Licensean Conditions (https://onlinelibrary.wiley.com/terms-and-conditions) on Wiley Online Library for rules of use; OA articles are governed by the applicable Creative Commons Licensean Conditions (https://onlinelibrary.wiley.com/terms-and-conditions) on Wiley Online Library for rules of use; OA articles are governed by the applicable Creative Commons Licensean Conditions (https://onlinelibrary.wiley.com/terms-and-conditions) on the applicable Creative Commons (https://onlinelibrary.wiley.com/terms-and-conditions) on the applicable Creative

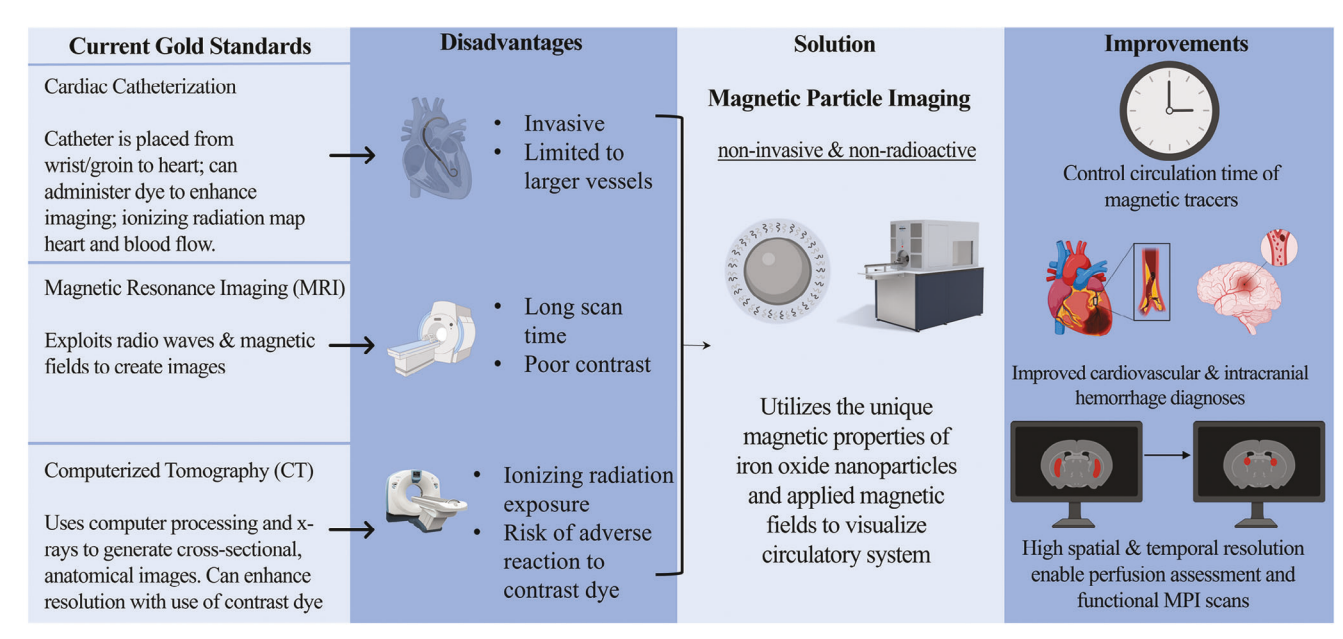


Figure 1. Current techniques to visualize blood circulation have limitations regarding patient risk, temporal resolution, and spatial resolution. Magnetic particle imaging (MPI) is a novel imaging modality that has the potential to address some of the clinical limitations facing the imaging of blood circulation, aiding in diagnosis of cardiac disease and vascular injury while also enabling perfusion studies and direct functional scans.^[7–9]

undergone refinement and improvement over the past century and remains one of the most frequently performed procedures in the United States for the diagnosis and treatment of vessel blockages. Through the thin catheter, clinicians can take biopsies, administer therapeutics, and address arterial blockages by placing stents to ensure vessel patency. Visualizing the vessel while providing an intervention is not possible with noninvasive imaging techniques, underscoring the continued significance of catheterization techniques in modern clinical settings.

Initially limited to larger blood vessels and heart chambers, cardiac catheterization has improved with technological and safety advancements to visualize smaller vessels, facilitated by novel image processing methods such as digital subtraction angiography (DSA).^[11] This process enables visualization of millimeter-scale vessels by capturing a time series of images as a bolus of contrast agent is delivered. The subtraction of the image series allows for following the bolus flow through vasculature over time. While there are minor risks of blood clot formation or arrhythmias associated with the procedure, such complications are rare. Similarly, allergic reactions to contrast agents are infrequent, making this procedure and visualization technique common practice.

As equipment and reconstruction algorithms are continuously refined, higher resolution images are produced while also limiting scan time and ionizing radiation exposure. However, catheterization can pose greater risks for patients with existing conditions or comorbidities. For example, patients with congenital anomalies or congenital heart conditions that alter vessel size or structure may be at heightened risk for complications such as blood clots or vessel damage. The risk is also elevated for patients with cardiac disease who have developed collateral vessels in response to artery blockages or atherosclerotic plaques.

Like cardiac catheterization procedures, peripheral vascular angiography is a catheter-based procedure often performed on

the large arteries in the legs. A contrast agent is delivered to peripheral arteries via a catheter to enable diagnosis of peripheral artery disease (PAD) or identification of blockages or injury. Like cardiac catheterization, the build-up of the contrast agent delivered via the catheter can be visualized via X-ray to show the development of plaques or identify blocked arteries in the extremities. Success of this procedure depends on the size and accessibility of the vessels, as well as any challenges posed by vessel injury or vessel tortuosity. Risks with peripheral vascular angiography are like cardiac catheterization procedures and remain low when performed on patients without comorbidities.

1.2. Ventriculography for Diagnosis of Cardiac Disease

Ventriculography, often known as a multigated acquisition scan (MUGA), blood pool imaging, or a blood pool scan, is the assessment of heart chamber pressures throughout the cardiac cycle (e.g., a right heart ventriculography assessment measures pressures in the right atrium and right ventricle). Traditionally, catheter-based measurements of pressures in the heart chambers are coupled with catheter delivery of contrast agents for coupled assessments with noninvasive imaging techniques. [12] As noninvasive imaging techniques have improved in precision while having fewer risks, the recommendation for use of catheter-based ventriculography has declined over the last decade. [13,14]

1.3. Noninvasive Ventriculography for Diagnosis

Noninvasive cardiac ventriculography or blood pool scans, without the use of catheterization, are used to visualize and diagnose coronary artery disease or heart failure based on the pooling of blood in the heart chambers during a cardiac cycle. These

21925259, 0, Downloaded from https://onlinelibrary.wiley.com/doi/10.1002adm.m.202400612 by University Of Flordat, Wiley Online Library for rules of use; OA articles are governed by the applicable Creative Commons Licensens and Conditions (https://onlinelibrary.wiley.com/remrs-and-conditions) on Wiley Online Library for rules of use; OA articles are governed by the applicable Creative Commons Licensens and Conditions (https://onlinelibrary.wiley.com/remrs-and-conditions) on Wiley Online Library for rules of use; OA articles are governed by the applicable Creative Commons Licensens and Conditions (https://onlinelibrary.wiley.com/remrs-and-conditions) on Wiley Online Library for rules of use; OA articles are governed by the applicable Creative Commons Licensens and Conditions (https://onlinelibrary.wiley.com/remrs-and-conditions) on Wiley Online Library for rules of use; OA articles are governed by the applicable Creative Commons Licensens and Conditions (https://onlinelibrary.wiley.com/remrs-and-conditions) on Wiley Online Library for rules of use; OA articles are governed by the applicable Creative Commons Licensens and Conditions (https://onlinelibrary.wiley.com/remrs-and-conditions) on Wiley Online Library for rules of use; OA articles are governed by the applicable Creative Commons Licensens and Conditions (https://onlinelibrary.wiley.com/remrs-and-conditions) on the conditions are governed by the applicable Creative Commons and Conditions are governed by the applicable Creative Commons and Conditions are governed by the applicable Creative Commons are governed by the applicable Creati



noninvasive imaging strategies can often be coupled with catheter-based procedures (angiography or ventriculography), but the labeling and contrast agent delivery are often performed differently. In these noninvasive procedures, a contrast agent, such as a radioactive dye, is used to label red blood cells and the procedure is commonly referred to as radionuclide ventriculography.[15] Labeled cells are typically introduced to the body using ex vivo labeling since a catheter is not used to deliver the contrast agent locally. Blood is drawn from the patient, red blood cells are labeled outside of the body in the laboratory, and then these labeled cells are reintroduced to the body. [16] Clinically, the most common technique to label red blood cells employs radiopharmacology agents which allow one to track emitted ionizing radiation with a gamma imager or single-photon emission computed tomography (SPECT).[17] However, recent investigations and assessment of patient data suggest that validation via other planar imaging modalities, such as magnetic resonance imaging (MRI), may improve diagnostic assessments in patients with congenital defects or abnormal ventricle function.[14,18,19] When a person has coronary artery disease, heart failure, or altered heart function, blood will pool in the heart chambers and this signal is detected at different stages of the cardiac cycle by visualizing the accumulation of the ionizing radiation within the heart chamber. While this technique is also relatively commonplace in hospitals, patients with additional complications or underlying conditions are at greater risk. Pregnant women are unable to undergo these types of assessments, as the radiopharmaceutical used may pose a threat to the fetus. In addition, patients with hampered kidney function or kidney disease may be advised against these procedures as the radiopharmaceutical is usually filtered from the blood stream via the kidneys and may pose an unnecessary risk to the patient.

1.4. Visualizing Internal Bleeding via Ultrasound and Magnetic Resonance Imaging (MRI)

While imaging and diagnostic tools, despite their complexities, have been optimized for diagnosing cardiac disease, similar advancements have not been made for other clinical indications, such as aneurysms, internal trauma, and internal hemorrhage. For example, strokes occur when oxygen delivery to the brain is disrupted. Hemorrhagic strokes make up about 13% of stroke cases, where a vessel in the brain ruptures, preventing oxygen delivery and leading to blood pooling at the site of rupture. Like a ruptured cerebral aneurysm, the resulting brain bleed and associated clots can put pressure on the brain tissue, causing further damage to the surrounding tissues. Diagnosis of a brain bleed often occurs via MRI, which can detect brain bleeds and ischemic injury, when performed soon after the event. However, the resolution of these images can pose challenges in early diagnosis, even with the use of contrast agents or tracers.

Other conditions and diseases that lead to internal bleeding include a rising number of conditions affecting women's health, such as endometriosis. Usually, a conditional endometriosis diagnosis results from a combination of ultrasound imaging and MRI,^[20] as the penetration depth and resolution of MRI is substantially better than a transvaginal ultrasound. MRI can often detect large endometriosis lesions but cannot routinely detect superficial peritoneal implants.^[21,22] However, final diagnosis and

potential treatment requires laparoscopic surgery. Further characterization of other disease phenotypic structures, such as hemorrhagic cysts, involve visualization via ultrasound imaging, however laparoscopic surgery is still required for final diagnosis.^[23]

Internal bleeding can also occur via an aneurysm in any tissue, including the intestinal tract. Diagnosis and location of gastrointestinal bleeds is complex, usually involving multiple modalities including endoscopy, computed tomography (CT), and catheterbased angiography. In extreme cases exploratory surgery is required for treatment and diagnosis. Noninvasive diagnostic tools with improved penetration depth and mitigation of tissue background signal are needed to limit the number of invasive procedures performed and in cases where invasive procedures are still necessary, to provide surgical teams with more detailed knowledge of the repair needed before in surgery.

1.5. Opportunities for Future Advancement

Techniques with improved temporal resolution and limited signal attenuation are needed. Improved resolution can be achieved by the design of novel imaging modalities, improved detection and reconstruction algorithms, or the optimization of contrast agent or tracer designs.[8,25] In recent decades researchers and clinicians have moved toward noninvasive imaging modalities for blood pool imaging. This involves the administration of a contrast agent or tracer that modulates an input signal, leading to observable differences by a detector. These diagnostic imaging tools are referred to as tracer imaging tools and can often be paired with structural imaging tools such as CT or MRI to resolve the location of the tracer relative to anatomical features. Current and emerging imaging modalities for tracking blood flow and internal bleeding are summarized in Table 1. Techniques such as ultrasound, [26] positron emission tomography (PET),[27] SPECT,[28] and magnetic resonance angiography (MRA)[29] are all used clinically for angiography applications. However, the cardiac catheterization procedure remains the most popular, with >1 000 000 procedures performed in the United States annually.[9] Techniques such as ultrasound and optical imaging have shown promise in noninvasive angiography; however, limited penetration depth poses challenges in diagnosing internal bleeding.[30] Tools with improved penetration depth, such as CT and MRI, are applied to various clinical indications such as ischemic stroke, aneurysm, and heart disease, offering enhanced resolution when paired with a contrast agent. Challenges such as long acquisition times, deconvolution of contrast agent signal from other features, and high doses of ionizing radiation motivate continued research into CT and MRI for blood-related diagnostics.[31] While research on optimizing contrast agents for CT and MRI is active, [32-35] in this review, we will focus on MPI and its application in imaging blood circulation.

MPI is an imaging modality in which signal generation is based on the dynamic magnetization of superparamagnetic iron oxide nanoparticle (SPION) in an applied alternating magnetic field. This makes MPI unique among imaging modalities because signal is generated solely from the unique physics of nanomaterials, resulting in negligible background signal due to surrounding features. In MPI, a selection magnetic field gradient is applied opossing a uniform alternating magnetic field, creating small field free region (FFR), surrounded by a region with

ADVANCED HEALTHCARE MATERIALS

21925259, 0, Downloaded from https://onlinelibrary.wiley.com/doi/10.1002adm.m.202400612 by University Of Flordat, Wiley Online Library for rules of use; OA articles are governed by the applicable Creative Commons Licensens and Conditions (https://onlinelibrary.wiley.com/remrs-and-conditions) on Wiley Online Library for rules of use; OA articles are governed by the applicable Creative Commons Licensens and Conditions (https://onlinelibrary.wiley.com/remrs-and-conditions) on Wiley Online Library for rules of use; OA articles are governed by the applicable Creative Commons Licensens and Conditions (https://onlinelibrary.wiley.com/remrs-and-conditions) on Wiley Online Library for rules of use; OA articles are governed by the applicable Creative Commons Licensens and Conditions (https://onlinelibrary.wiley.com/remrs-and-conditions) on Wiley Online Library for rules of use; OA articles are governed by the applicable Creative Commons Licensens and Conditions (https://onlinelibrary.wiley.com/remrs-and-conditions) on Wiley Online Library for rules of use; OA articles are governed by the applicable Creative Commons Licensens and Conditions (https://onlinelibrary.wiley.com/remrs-and-conditions) on Wiley Online Library for rules of use; OA articles are governed by the applicable Creative Commons Licensens and Conditions (https://onlinelibrary.wiley.com/remrs-and-conditions) on the conditions are governed by the applicable Creative Commons and Conditions are governed by the applicable Creative Commons and Conditions are governed by the applicable Creative Commons are governed by the applicable Creati

Table 1. Main features of current and emerging noninvasive imaging modalities utilized in imaging of the circulatory system.^{136,37}1

Imaging modality	Excitation modality	Quantitative? (Yes/No)	Anatomical? (Yes/No)	Spatial resolution	Temporal resolution	Penetration depth	Imaging agents	Patient risk	Cost
Ultrasound	Sound waves	°N	Yes	10–100 µm	s-min	50 cm	Microbubbles	Heat and cavitation	Low
Computed tomography (CT)	X-rays	Yes	Yes	25–200 µm	s-min	Whole body imaging	lodine	Radiation	Low/Med
Positron emission tomography (PET)	Gamma radiation	Yes	°N	4–5 mm	s-min	Whole body imaging	Radioactive tracers	Radiation	High
Single-photon emission computed tomography (SPECT)	Gamma radiation	Yes	° Z	0.5–2 mm	E E	Whole body imaging	Radioactive tracers	Radiation	Med
Magnetic resonance imaging (MRI)	Magnetic fields	Yes	Yes	25–100 μm	min-h	Whole body imaging	Gadolinium, iron oxide particles	Heat, peripheral nerve stimulation, metal/magnetic implants	High
Magnetic particle imaging (MPI) ^{a)}	Magnetic fields	Yes	°Z	1–3 mm, as low as 150 μm ^[38]	ms-min	Whole body imaging	Iron oxide particles	Heat, peripheral nerve stimulation, metal/magnetic implants	Med

a strong magnetic field. Tracers outside of the FFR are saturated and only weakly respond to the alternating magnetic field, while those inside the FFR respond strongly. The magnetization of SPI-ONs in the FFR oscillates as a response to the alternating magnetic field. This change is detected by pickup coils and results in a signal that is proportional to the local SPION concentration. By moving the FFR to cover a region of interest, a quantitative 3D distribution of SPIONs can be captured.

The limited presence of background signal combined with the penetration depth of MPI can make imaging of vessel structures within the peritoneal cavity possible and potentially reduce the need for invasive diagnostic procedures. Additionally, the impressive temporal resolution and direct signal generation in MPI can make functional perfusion assessment possible. In this review, we identify the current state of MPI technology development for key applications in cardiac disease diagnosis, diagnosis of brain bleeds, and identification of sites of internal bleeding in key tissues such as the lungs and kidneys. We also identify other sites of internal bleeding resulting from disease or injury that may benefit from the high spatial and temporal resolution afforded by MPI.

2. MPI as an Emerging Diagnostic Imaging Modality

MPI is a new imaging technique well suited to contribute to the diagnosis of altered blood flow, vascular injury or blockage, pooling of blood, and internal bleeding.^[8] MPI uses SPIONs as tracers. SPIONs can be readily located and quantified using MPI-based on their magnetic behavior. To visualize the SPION tracers, an external alternating magnetic field is applied, leading to the nonlinear magnetization of the SPIONs. Nonlinear magnetization allows for detection of the magnetic moment, which is orders of magnitude more intense than nuclear moments resulting from radiographic tracers used to enhance signals in MRI. MPI has a theorized spatial resolution on the sub-mm scale, a temporal resolution on the millisecond scale, as well as full body penetration with little to no tissue background.^[39]

To achieve this theorized resolution, optimized SPION tracers are required, with a detailed understanding of their response to dynamic oscillating magnetic fields. [2] The application of tracer imaging tools to replace or augment current angiography or ventriculography techniques means that the SPION tracer must remain in circulation over the duration of the image acquisition. Thus, the design of SPION tracers with controlled circulation time is a critical feature for the clinical realization and application of this technique. Furthermore, it is imperative that we understand how SPION tracer parameters impact their sites of accumulation and image resolution.

First, biodistribution and pharmacokinetic assessments must be carried out to understand the performance of SPION tracers administered into systemic circulation that are then intended to serve as tracers for blood circulation imaging. There are both direct and indirect methods for assessment of blood half-life of imaging tracers. [40,41] A robust direct technique to quantify circulation half-life is to radiolabel particles and to have blood draws over time in which the circulating concentration is determined. Alternatively, blood circulation half-life may be determined indirectly by imaging vessels and determining when the signal has decayed. This method requires only periodic imaging; however,

⁴ Indicates imaging modality is in the preclinical stages of development

half-lives near 7 h by monitoring the MPI signal in the heart and

10 kDa PEGylated formulation was found to have a blood half-life of ≈60 min. This was found in a rat model and by monitoring the signal to noise ratio with MRI.[56] Another study generated particles with ≈20 nm core diameters and PEGylated the surface with 5 kDa PEG. In their mouse model, they determined blood

fitting to a one compartment model.[44] These studies all show great promise for tracers that can be used in blood pool imaging as well as other applications. However, there is a lack of consistency in the methods of determining half-life across studies. When examining the current scope of tracers that may be used for blood pool imaging, one notices that there are very few tracers designed for optimal signal generation, and a spectrum of clearance times. This idea can be visualized in Figure 2, where there are no tracers in the upper right corner of the plot, which represents both high sensitivity and circulation time (raw data and references are provided in Table 4). To use MPI across clinical applications, it is important to consider that differing clearance times would be desirable in disparate situations and that continued improvement of resolution in MPI is important. As the field advances to fill these gaps, many researchers have performed preclinical studies across organ systems to show potential applications of MPI in blood pool imaging. Below we

discuss progress in the use of MPI in cardiac, cerebral, and gen-

eral organ perfusion imaging both in vitro using phantoms and

related to tracer concentration. In this context, it is important for researchers to consider and carefully report the analysis being conducted to determine circulation time in their studies. For the research discussed herein that describes the design of longcirculating tracers for blood pool imaging using MPI, this distinction will be reported. Moreover, it is important to recognize that radiolabeling, like any surface modification, may impact the overall half-life independent of the SPION itself, in turn complicating the assessment.

it is dependent on the imaging set-up in use. MPI offers an advantage in the use of this method since the signal is linearly cor-

2.1. Optimizing MPI Tracers for Imaging of Blood Pooling and Circulation

One of the first major hurdles to overcome in the use of MPI for applications in cardiac and vascular diagnoses is the design of an optimized tracer from both a circulation time and a signal generation perspective. There are several commercially available tracers that can be used in MPI (Table 2), including ones that are approved clinically as an MRI contrast agent (Resovist, Bayer, Germany) or an iron supplement (Feraheme, Covis Pharma, Switzerland). Resovist, also known by the generic name ferucarbotran, works to generate a signal in MPI, however it is not optimal for vascular applications due to the product's large polydispersity and rapid clearance. [42,43] In many of the studies discussed herein, ferucarbotran is used as a benchmark for comparison.

Work has been done to optimize MPI tracers for numerous biomedical applications outside of blood pool imaging alone. [7,51,52] Recent works that focused on optimizing the circulation time of carriers for blood pool imaging attempted to leverage the long circulation time of red blood cells.^[53,54] By utilizing changes in the salinity of a particle suspension, researchers were able to load human red blood cells with ferucarbotran and characterize their magnetic properties. Additionally, the researchers performed an in vivo study with injection of murine red cells loaded with ferucarbotran. This was followed by blood collection and magnetic particle spectroscopy (MPS) to assess circulation time. They determined that the red blood cell tracers had a halflife of ≈ 3 h as opposed to free ferucarbotran, which is cleared in the order of minutes. [35] In a later study, the same approach showed that the red cell based tracer could lead to reliable detection of events such as breathing and the heartbeat.^[53] These results are promising for the future of red blood cell based MPI tracers. However, they are limited in scope since ferucarbotran is not optimized for signal generation and most of the measurements were not significantly above the noise level after 3 h.

Other groups have explored the use of stealth polymers to improve tracers for MPI of the blood pool (Table 3).[44,55,56] The most common stealth polymer employed for this purpose is PEG. Khandhar et al. developed a tracer termed LS-008 which has a ≈25 nm core diameter with 20 kDa PEG loaded at ≈18 mol% on the surface. [55] They also used a mouse model, where after injection, blood draws and MPS were performed to determine circulation time. They determined that LS-008 had a blood halflife of 108 min. [55] A separate study investigated the use of PE-Gylated multicore particles. They tested varying PEG molecular weights and stoichiometries and while some were not stable, a

3. Applications of MPI for Specific Clinical **Indications**

in vivo in small animal models.

Since the circulatory system is involved across all organ systems, the use of blood pool imaging has many applications including the ability to detect and diagnose cardiac/vascular disease, cerebral hemorrhages/hemorrhagic stroke, other internal hemorrhage, as well as to assess organ perfusion. Organ perfusion can be used in functional imaging, which concerns monitoring the changes in flow as a result of the patient performing a certain function (speaking, thought exercise etc.), and can be used in brain mapping and the diagnosis of disease. In the following sections we highlight organ systems for which MPI blood pool imaging has demonstrated pre-clinical success.

3.1. MPI in Cardiac Imaging and Assessment of Cardiac Function

One major purpose of blood pool imaging is monitoring and quantifying blood flow as it can highlight changes due to heart disease, stenosis and cardiac dysfunction (Figure 3A). Researchers have demonstrated that MPI-based imaging of circulation can generate signal at relevant flow rates and detect disease characteristic structures/flow alterations^[61–70] (**Table 5**). For the quantification to be accurate and helpful in these applications, the temporal resolution of the imaging technique must be sufficiently shorter than the time dependency of what is being measured. In one study, continuous data streaming and flexible reconstruction frameworks were used to achieve MPI of 40 cm s⁻¹ flow in a phantom with a commercially available Perimag tracer and a traveling wave MPI scanner. [64] While this is similar to venous blood flow, faster speed would be necessary for flow near

ADVANCED HEALTHCARE MATERIALS

Table 2. Properties and status of clinical and preclinical superparamagnetic iron oxide nanoparticle (SPION) formulations that have been used in magnetic particle imaging (MPI).

Generic Name: Company and Brand name	Coating	Hydrodynamic Diameter [nm]	Core diameter [nm]	Half-Life	Application(s)	Status	Refs.
FERUCARBOTRAN: RESOVIST & CLIAVIST. CLINICAL BRAND NAMES FOR FERUCARBOTRAN (BAYER, GERMANY)- PRODUCTION NOT ACTIVE VIVOTRAXTN: FERUCARBOTRAN BRANDED FOR MPI (MAGNETIC INSIGHT, CALIFORNIA USA)	Carboxydextran	62	Multicore, ≈4 nm per core	≈35 min in mice	Magnetic resonance imaging (MRI) contrast agent	Clinically approved in Japan and other limited countries. Recommended dose 0.45–0.7 mmol Fe	[44, 45]
FERUMOXYTOL: FERAHEME (COVIS PHARMA, SWITZERLAND) FORMERLY RIENSO	Carboxymethyl-dextran	30	3-4 nm	≈14 h in humans	Iron supplementation and MRI angiography	FDA approved as iron supplement with box warning. Recommended dose 1 g Fe over 3–8 days. (Feraheme) withdrawn from EU (Rienso)	[8, 46, 47]
FERASPINTM: (NANOPET PHARMA, GERMANY) FORMERLY MANUFACTURED AT: MILTERI BIOTECH, GERMANY	Carboxydextran	Formulations give tunable sizes ranging from 10-70 nm	Multicore, 5–7 nm per core	Size-dependent range, not specified	MRI blood pool agent	Commercially available for research (not for human use)	[48]
PERIMAG: MICROMOD, GERMANY	Dextran	130	Multicore, ≈5.5 nm per core	≈20 min in mice	MRI contrast agent	Commercially available for research (not for human use)	[49]
PRECISIONMRX: IMAGION BIOSYSTEMS, SAN DIEGO USA	mPEG	41	24–25 nm	Not specified	MRI contrast agent	Commercially available for research (not for human use)	[20]
SYNOMAG-D: MICROMOD, GERMANY	Dextran	56	Multicore, 5–15 nm per core	0.62 h in mice	Hypothermia	Commercially available for research (not for human use)	[44]

Table adapted with permission.¹³⁷1 Copyright 2022, Royal Society of Chemistry.

21926259, 0, Downloaded from https://onlinelibitary.wiley.com/doi/10.1002adm.202408612 by University Of Florida, Wiley Online Library on [01/07/2024]. See the Terms and Conditions (https://onlinelibrary.wiley.com/terms-and-conditions) on Wiley Online Library for rules of use; OA articles are governed by the applicable Creative Commons. License

21922659, 0, Downloaded from https://onlinelibrary.wiley.com/doi/10.1002/adhm.202400612 by University Of Florida, Wiley Online Library on [01/07/2024]. See the Terms and Conditions (https://online.com/doi/10.1002/adhm.202400612 by University Of Florida, Wiley Online Library on [01/07/2024]. See the Terms and Conditions (https://online.com/doi/10.1002/adhm.202400612 by University Of Florida, Wiley Online Library on [01/07/2024]. See the Terms and Conditions (https://online.com/doi/10.1002/adhm.202400612 by University Of Florida, Wiley Online Library on [01/07/2024]. See the Terms and Conditions (https://online.com/doi/10.1002/adhm.202400612 by University Of Florida, Wiley Online Library on [01/07/2024]. See the Terms and Conditions (https://online.com/doi/10.1002/adhm.202400612 by University Of Florida, Wiley Online Library on [01/07/2024]. See the Terms and Conditions (https://online.com/doi/10.1002/adhm.202400612 by University Of Florida, Wiley Online Library on [01/07/2024]. See the Terms and Conditions (https://online.com/doi/10.1002/adhm.202400612 by University Of Florida, Wiley Online Library on [01/07/2024]. See the Terms and Conditions (https://online.com/doi/10.1002/adhm.202400612 by University Of Florida, Wiley Online Library on [01/07/2024]. See the Terms and Conditions (https://online.com/doi/10.1002/adhm.202400612 by University Of Florida, Wiley Online Library on [01/07/2024]. See the Terms of the University Of Florida (https://online.com/doi/10.1004).

onlinelibrary.wiley.com/terms-and-conditions) on Wiley Online Library for rules of use; OA articles are governed by the applicable Creative Commons License

Table 3. Summary of recent studies investigating the development of long-circulating tracers designed for application in magnetic particle imaging (MPI).

Adv. Healthcare Mater. 2024, 2400612

Tracer Core diameter Coating Hydrodynamic diameter Zeta potential In vivo characterization Blood half-life Refs. Resovist loaded \$								
wist loaded	Tracer	Core diameter	Coating	Hydrodynamic diameter	Zeta potential	In vivo characterization	Blood half-life	Refs.
20 kDa PEG	Resovist loaded RBCs	≈4 nm	RBC	≈7 µm (red blood cell carrier) 62 nm (Resovist)	Not reported	Blood half-life assessed following tail vein injections using blood draws and MPS in mice	3 h in mice	[53]
.PEG10K2 Multicore (≈40 nm) PEG (varying 84 nm —3.4 mV Blood half-life assessed by signal monitoring 62 min in rats MW) rats following tail vein injections 20.7–22.6 nm 5 kDa PEG 54–76 nm —7.6 mV Blood half-life assessed following tail vein mice	RS-008	25 nm	20 kDa PEG	≈80 nm	–4.5 mV	Blood half-life assessed following tail vein injections using blood draws and MPS in mice	108 min in mice	[55]
20.7–22.6 nm 5 kDa PEG 54–76 nm –7.6 mV Blood half-life assessed following tail vein 6.99 h in mice injections using MPI signal in mice	MCP-PEG10K2	Multicore (≈40 nm)	PEG (varying MW)	84 nm	–3.4 mV	Blood half-life assessed by signal monitoring with magnetic resonance imaging (MRI) in rats following tail vein injections	62 min in rats	[56]
	RL-1	20.7–22.6 nm	5 kDa PEG	54–76 nm	–7.6 mV	Blood half-life assessed following tail vein injections using MPI signal in mice	6.99 h in mice	[44]

500 **Blood Half Life [min]** RL-1 400 300 200 eraspin ● LS-008 100 Svnomag-D Ferucarbotran 2 6 0 4 MPI Sensitivity/Sensitivity Ferucarbotran

Figure 2. Visual representation of circulation half-lives achieved in mice from papers reviewed compared to selected commercially available tracers discussed in Table 3. All magnetic particle imaging (MPI) sensitivity values have been normalized to that of ferucarbotran, shown in black. Green points represent tracers designed for MPI applications, and warmer colored points represent tracers compatible, but not specifically designed for MPI. The scarcity of datapoints portraying both high MPI sensitivity and blood half-life indicate potential for novel MPI tracer development. Values used in the figure and their sources are given in Table 4.

Table 4. Tabulated values for the data shown in Figure 2 along with the references from which the sensitivity half-life data are obtained.

Tracer	Circulation half-life in mice	Sensitivity/ sensitivity ferucarbotran	Refs.
Ferucarbotran	35 min	1	[44]
Feraheme	45 min	0.93	[57, 58]
FeraspinXS	30 min	_	[59]
FeraspinXXL	_	0.55	[60]
Perimag	19 min	0.47	[60, 49]
Precision MRX	_	0.98	[60]
Synomag-D	37 min	3.4	[44]
RL-1	420 min	3	[44]
LS-008	105 min	5	[55]

the aorta, which can reach hundreds of cm s⁻¹. A separate study sought to analyze if the temporal resolution of MPI allowed for the imaging of coronary artery flow (20–64 cm s⁻¹). Using Perimag and a Bruker preclinical scanner, they obtained agreement in determined flow velocities within $\approx\!20\%$ across 4- and 6-mm diameter phantoms. [66] These studies used separate scanning systems, which limit the ability to compare. Additionally, they avoided more complex phantom geometries to maintain laminar flow since it is easily calculable. However, this is not necessarily representative of the in vivo setting when extensive disease is present. One study sought to recapitulate some of the complexity seen in vivo in a phantom model by constructing a model of a carotid artery aneurysm. [71] This study used a styrene-magnetite tracer referred to as MM4 and a Bruker preclinical scanner. Similar pulsation rates were detected in MPI as with MRI.

In a related application, MPI was used to detect coagulation of blood ex vivo. [61] To induce coagulation, CaCl₂ was added to

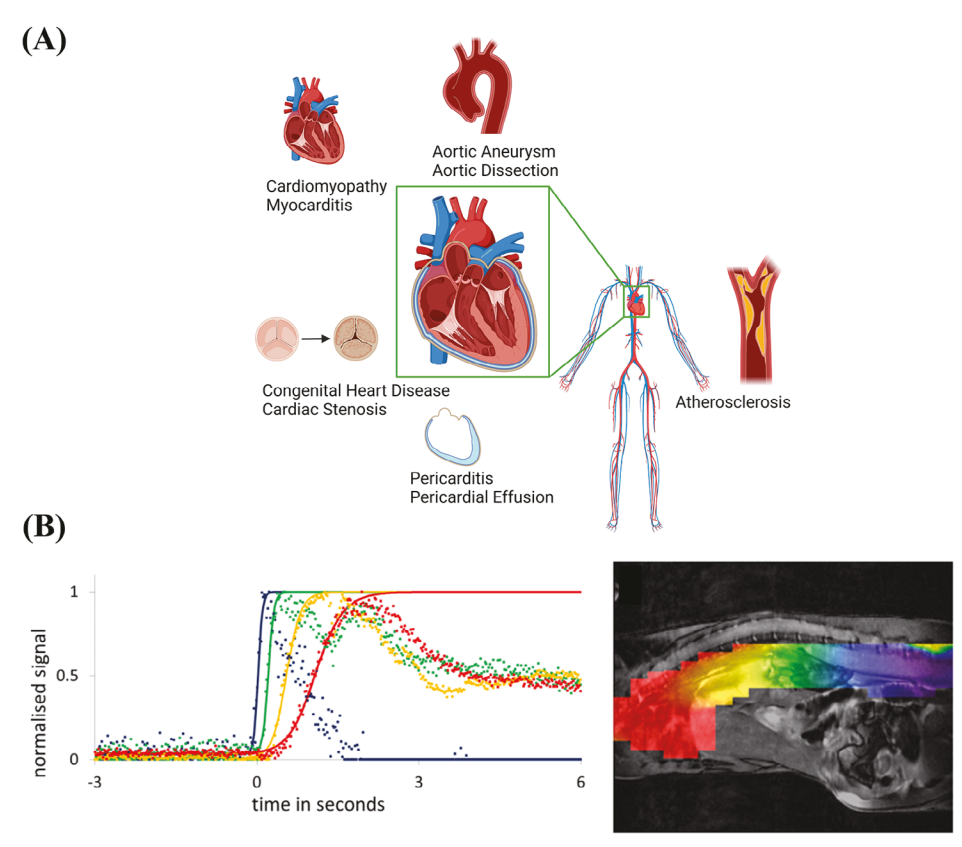


Figure 3. A) Clinical diagnoses related to the heart that could benefit from the use of blood pool imaging in diagnosis and/or treatment. Quantitative tracking of superparamagnetic iron oxide nanoparticles (SPIONs) can enable detecting disturbances in circulation including plaques, dissections, aneurisms, defects, etc. B) Demonstration of how magnetic particle imaging (MPI) can be used to visualize the movement of injected tracer (ferucarbotran) through the murine inferior vena cava following tail vein injection. This set of imaging led to the determination of blood velocities that show good agreement with those determined using magnetic resonance imaging (MRI), demonstrating the diagnostic potential of MPI. Images in Figure 3B are reproduced with permission. [62] Copyright 2018, IOP Publishing.

whole sheep's blood. The tracer M-300 and an in-house scanner were used. They found that coagulated blood displayed a decayed signal and attributed this to changes in viscosity, which impacts the relaxation of the tracer. The fact that differentially viscous environments led to distinct images intensities highlights the potential for multicontrast MPI. However, more optimization is needed, such that a coagulated signal is distinct from an area with a lower concentration of tracer.

In an in vivo study, researchers sought to measure blood velocities in a murine model. [62] They used ferucarbotran and a Bruker preclinical scanner. Phantom studies were done to calibrate the system before the in vivo experiment. The results were compared to MRI determined velocities near the inferior vena cava and there was good agreement (Figure 3B). In related applications, researchers have used MPI to detect vulnerable plaques associated with atherosclerosis. [72,73] While these works do not focus

Table 5. Summary of recent studies investigating the use of magnetic particle imaging (MPI) for imaging and assessment of cardiac health and function.

Imaged model	Tracer	Scanner	Findings	Refs.
Ex vivo coagulation in sheep blood	M-300	In-house	Signal drop in coagulated conditions	[61]
Stenosis phantoms	Resovist	Traveling wave MPI	MPI can accurately detect and grade vascular stenosis with improved accuracy at lower levels of stenosis	[63]
In vivo murine blood velocities	Resovist	Bruker Preclinical	Velocities in the inferior vena cava agreed with MRA velocities $\approx\!21\mbox{cm s}^{-1}$	[62]
Dynamic bolus phantom	Perimag	TWMPI	$40\ cm\ s^{-1}$ superparamagnetic iron oxide nanoparticle (SPION) velocity is detectable with optimized reconstruction	[64]
In vivo rat blood flow velocities	Resovist	Bruker Preclinical	A hybrid MPI/magnetic resonance imaging (MRI) scanner can accurately detect blood velocities	[65]
Canonical stenosis phantoms	Perimag	Bruker Preclinical	Velocities up to $64 \ \text{cm s}^{-1}$ in $4 \ \text{mm ID}$ tubes with 20% error	[66]

Studies span in vitro, ex vivo, and in vivo experiments demonstrating imaging capabilities as well as the quantitated values from image analysis.

Table 6. Summary of recent studies investigating the use of magnetic particle imaging (MPI) based blood pool imaging for assessment of cerebral health and function

Imaged model	Tracer	Scanner	Findings	Refs.
Rat closed skull TBI	LS-13	Berkeley FFP	Injury and hematoma are visible immediately and 3 days later	[74]
Stroke model in mice	LS-008	Bruker Preclinical	MPI can be used for real time detection of perfusion deficits associated with ischemic stroke due to temporal resolution	[75]
Stroke phantom	Perimag	Novel MPI head scanner	A scanner can be constructed that can scan a human scale head at a temporal resolution of 2 frames s^{-1} and a detection limit of $\approx\!2~\mu g$ Fe	[76]
Intracranial hemorrhage model in mice	Perimag, Synomag-D	Bruker Preclinical	Using Synomag-D, the bleed can be detected in 3 min. Quantified at $0.003-0.06~\mu L~s^{-1}$ Multicontrast MPI can differentiate clotted blood from active bleeding	[81]
Healthy rhesus macaque	Mag3200 (PEG coated 20 nm core superparamagnetic iron oxide nanoparticles (SPIONs))	Novel handheld MPI head scanner	A novel scanner detects as little as 125 ng iron and enables the in vivo detection of SPIO concentration changes in a nonhuman primate brain. Represents a step toward functional imaging using MPI at scale	[78]

Studies demonstrate potential application of MPI in the diagnosis of stroke, traumatic brain injury (TBI), cerebral hemorrhage, and functional imaging.

on imaging a tracer in the blood stream, the end diagnostic goal is similar. Tong et al. suggested that intraplaque hemorrhaging could be detected using MPI without the use of a tracer.^[73] This study highlights the wide breadth of approaches that MPI enables in the cardiac diagnostic space. Most of the studies described in this section used nonoptimized tracers for analysis (Table 4). Additionally, most of them were done using phantoms. As the field continues to move forward, more ex vivo and in vivo studies are necessary to support evaluation of potential clinical translation.

3.2. Application of MPI in the Assessment of Cerebral Injury

MPI is theorized to enable the detection and diagnosis of several brain related injuries and pathologies based on the behavior of the tracer in the blood pool. The possible applications include detection of cerebral bleed, detection of ischemic stroke, and detection of intracranial hemorrhage (**Figure 4A**). Several studies have been carried out recently to demonstrate the feasibility of using MPI for these applications (**Table 6**).^[74–80]

In a study to assess the potential to detect traumatic brain injury, tracer LS-13 was used ($t_{1/2} = 4-6$ h).^[74] A rat model was subjected to a closed skull impact after administration of the tracer. Positive MPI signal was observed in the impacted area immediately following the injury and on day 3. In the injury group, the overall clearance of the tracer was slowed significantly by the accumulation at the injury site. The possibility of tracer accumulation in the brain is a possible concern and warrants a longer study that confirms eventual clearance of the tracer. Additionally, this model lacks clinical relevance since the tracer was administered before injury. Additional studies are necessary that more closely simulate clinical situations.

In a related and recent study, an intracranial hemorrhage in a C57BL/6 mouse model was induced through the administration of collagenase.^[81] In this study, when Perimag was administered via tail vein injection shortly following the hemorrhage induction the hemorrhage was not detected after 60 min due to the rapid clearance of Perimag. In contrast, when using the tracer

Synomag-D ($t_{1/2} = 60 \text{ min}$), the bleed was detected within 3 min. The rate of the bleed was also quantifiable (0.003 μ L min⁻¹). Additionally, they were able to take advantage of multicontrast MPI to distinctly visualize coagulated blood and active bleeding simultaneously. Multicontrast MPI was based on viscosity differences in the fluid and represents exciting new directions of MPI to aid in surgical or treatment decision making. In a separate study, MPI was used to monitor the development of a stroke. [75] In a murine model, blood flow to the middle cerebral artery was restricted. The tracer LS-008 was used in concert with a Bruker preclinical scanner and the cerebral blood fractions detected by MPI and MRI in both perfused sites (Figure 4B) and ischemic sites (Figure 4C) were similar (\approx 90%). Critically, the perfusion and vascular anatomy was imaged and visible within seconds using MPI. The main advantage for this application is the improved temporal resolution of MPI.

3.3. Application of MPI and Functional MPI (fMPI) in Assessment of Organ Perfusion

The spatial resolution and sensitivity of MPI makes it a suitable candidate for monitoring organ perfusion. For example, high spatial resolution makes possible the early detection of bleeds and detection of minor bleeding (Figure 5A). MPI of perfusion has been assessed in several organs in rodent models^[69,82–85] (Table 7), in addition to a human-sized model. [69] In one study that utilized the LS-008 tracer and compared to ferucarbotran, it was found that when LS-008 was injected into the blood pool of healthy FVB mice, the aorta was uniquely discernable and liver vessel and cranial vessel structure were all visible with LS-008 but not with ferucarbotran.^[82] In a separate study the perfusion of lungs was specifically analyzed.^[83] Imaging of the lungs is typically done via CT or X-ray since MRI performs poorly in this application. For targeting the lungs, the size of the tracer was increased. Specifically, SPIONs were coated in BSA and diameters of ≈20 µm were achieved. This led to over 80% of the signal being localized to the lungs after 10 min. However, the particle

21922659, 0, Downloaded from https://onlinelibrary.wiley.com/doi/10.1002/adhm.202400612 by University Of Florida, Wiley Online Library on [01/07/2024]. See the Terms and Conditions

and-conditions) on Wiley Online Library for rules of use; OA articles are governed by the applicable Creative Commons License

Table 7. Summary of recent studies investigating blood pool imaging using magnetic particle imaging (MPI) for assessment of internal organ perfusion and hemorrhage.

Imaged model	Tracer	Scanner	Findings	Refs.
Phantoms healthy mouse model	LS-008	Bruker Preclinical	LS-008 allows for MPI angiography of inferior vena cava and liver vessels, while Resovist does not	[82]
Rat lung perfusion model	MAA-superparamagnetic iron oxide nanoparticles (SPIOs)	In-house	SPIO cluster coated with BSA have a large size (20 um) allowing for rapid accumulation in the lungs and eventual RES clearance Resolution is similar to clinically used single-photon emission computed tomography (SPECT) scans	[37, 83]
A mouse model (Apc ^{Min/+}) predisposed to GI polyps given heparin to induce GI bleeding	LS-017	In-house	Circulation half-life determined by dynamic MPI signal was decreased from $\approx\!140$ to $\approx\!113$ min in the disease group indicated clearance through active bleeding. Bleeding rates found to be $\approx\!2-4~\mu L$ min $^{-1}$ via two separate models	[87]
Phantoms, rat model of hypercapnia	Unnamed 25 nm core PEG carboxyl coated	In-house single sided detector	The single sided system can dynamically track fCBV by MPI signal (10% change) as a function of hypercapnia. CNR $=$ 50	[77]
Respiratory cycle in mice	Perimag	Bruker Preclinical	MPI can accurately detect the pulmonary transit time of a bolus as well as the length of the respiratory rate.	[84]
3D printed small bowel phantom and ex vivo porcine small bowel	Perimag, LS-008	Bruker Preclinical	Single and multicontrast MPI using Perimag and LS-008 can detect leakage of tracer from the vascular compartment to the bowel lumen indicating feasibility for use in the visualization of gastrointestinal bleeding	[85]
Phantoms, rat model of hypercapnia	Synomag-D	Homebuilt FFL Scanner	Functional MPI (fMPI) time series can detect hemodynamic changes that occur as a result of alternating hyper/hypocapnia with high signal-to-noise-ratio	[67]
Oleic acid (acute) and bleomycin (chronic) induced lung injury in mice	Synomag-D	MOMENTUM scanner from Magnetic Insight	MPI can capture pulmonary vascular permeability in vivo. Heterogeneous injury is observable as opposed to only gaining information about the state of the lung barrier averaged across the entire lung	[86]

MPI enables quantification of internal hemorrhage as well as rapid perfusion assessments which can translate to functional imaging.

21922599, 0, Downloaded from https://onlinelibrary.wiley.com/doi/10.1002adhm.202400612 by University Of Florida, Wiley Online Library for rules of use; OA articles are governed by the applicable Creative Commons. Licenseand-conditions) on Wiley Online Library for rules of use; OA articles are governed by the applicable Creative Commons. Licenseand-conditions (https://onlinelibrary.wiley.com/terms-ad-conditions) on Wiley Online Library for rules of use; OA articles are governed by the applicable Creative Commons. Licenseand-conditions (https://onlinelibrary.wiley.com/terms-ad-conditions) on Wiley Online Library for rules of use; OA articles are governed by the applicable Creative Commons. Licenseand-conditions (https://onlinelibrary.wiley.com/terms-ad-conditions) on Wiley Online Library for rules of use; OA articles are governed by the applicable Creative Commons. Licenseand-conditions (https://onlinelibrary.wiley.com/terms-ad-conditions) on Wiley Online Library for rules of use; OA articles are governed by the applicable Creative Commons. Licenseand-conditions (https://onlinelibrary.wiley.com/terms-ad-conditions) on Wiley Online Library for rules of use; OA articles are governed by the applicable Creative Commons. Licenseand-conditions (https://onlinelibrary.wiley.com/terms-ad-conditions) on Wiley Online Library for rules of use; OA articles are governed by the applicable Creative Commons.

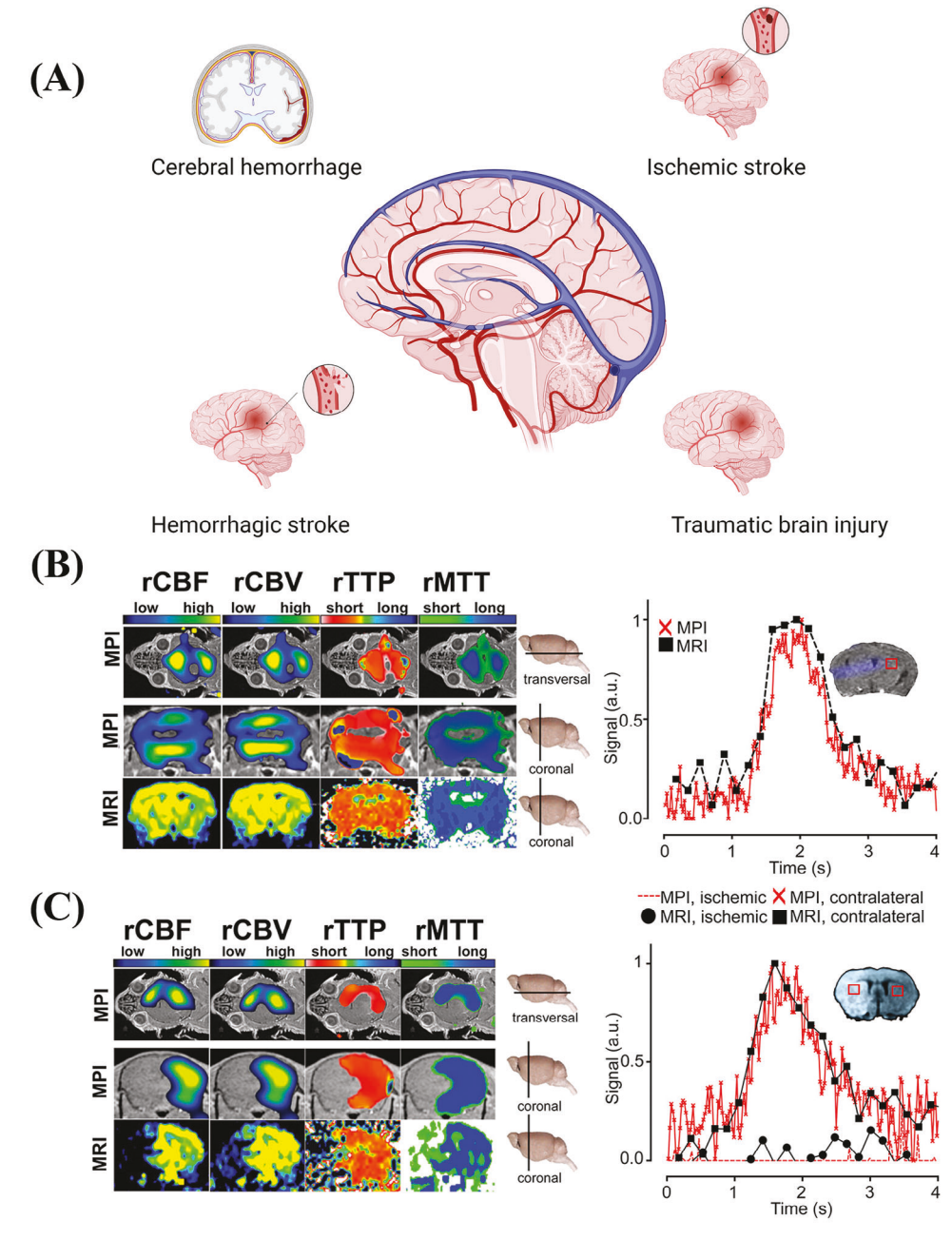


Figure 4. A) Clinical diagnoses that may benefit from the use of magnetic particle imaging (MPI) for visualization of blood flow in the brain due to improved temporal resolution and direct signal generation. B) An example of MPI-based imaging of cerebral perfusion in a healthy mouse. Similar signal curves and calculated perfusion maps for relative cerebral blood flow (rCBF), relative cerebral blood volume (rCBV), relative time to peak (rTTP), and relative mean transit time (rMTT) are observed in both MPI and magnetic resonance imaging (MRI). C) Demonstration of MPI image detection of ischemic stroke. Following the blockage of the medial cerebral artery and administration of LS-008 tracer, animals were imaged using both MPI and MRI. Clear differences in signal curves and calculated parameter maps were observed when comparing the ischemic left hemisphere to the perfused right. Signal curves were similar across MPI and MRI in both locations. This demonstrates the near real-time detection of perfusion deficits which can translate to improved stroke imaging, diagnosis, and treatment. Figure 4B,C is reproduced with permission. [75] Copyright 2017, American Chemical Society.

degraded and after 1 day primarily exited the lungs and was cleared again by the liver. This study shows the potential of optimization of various tracers for perfusion analysis of separate organs. MPI also holds promise in applications such as pulmonary vascular leakage detection. For example, Feng et al. demonstrated MPI-based detection of pulmonary vascular leakage heterogene-

ity across the lung in both acute and chronic lung injury models in mice. [86] A separate study sought to show that MPI could have angiographic applications in the imaging of perfusion of human-sized organs. To test this hypothesis, a porcine kidney perfusion apparatus was constructed and comparisons of MRA and MPI using ferucarbotran or Perimag were carried out. [69] Vessels within

21922659, 0, Downloaded from https://onlinelibrary.wiley.com/doi/10.1002/adhm.202400612 by University Of Florida, Wiley Online Library on [01/07/2024]. See the Terms

and-conditions) on Wiley Online Library for rules of use; OA articles are governed by the applicable Creative Commons License

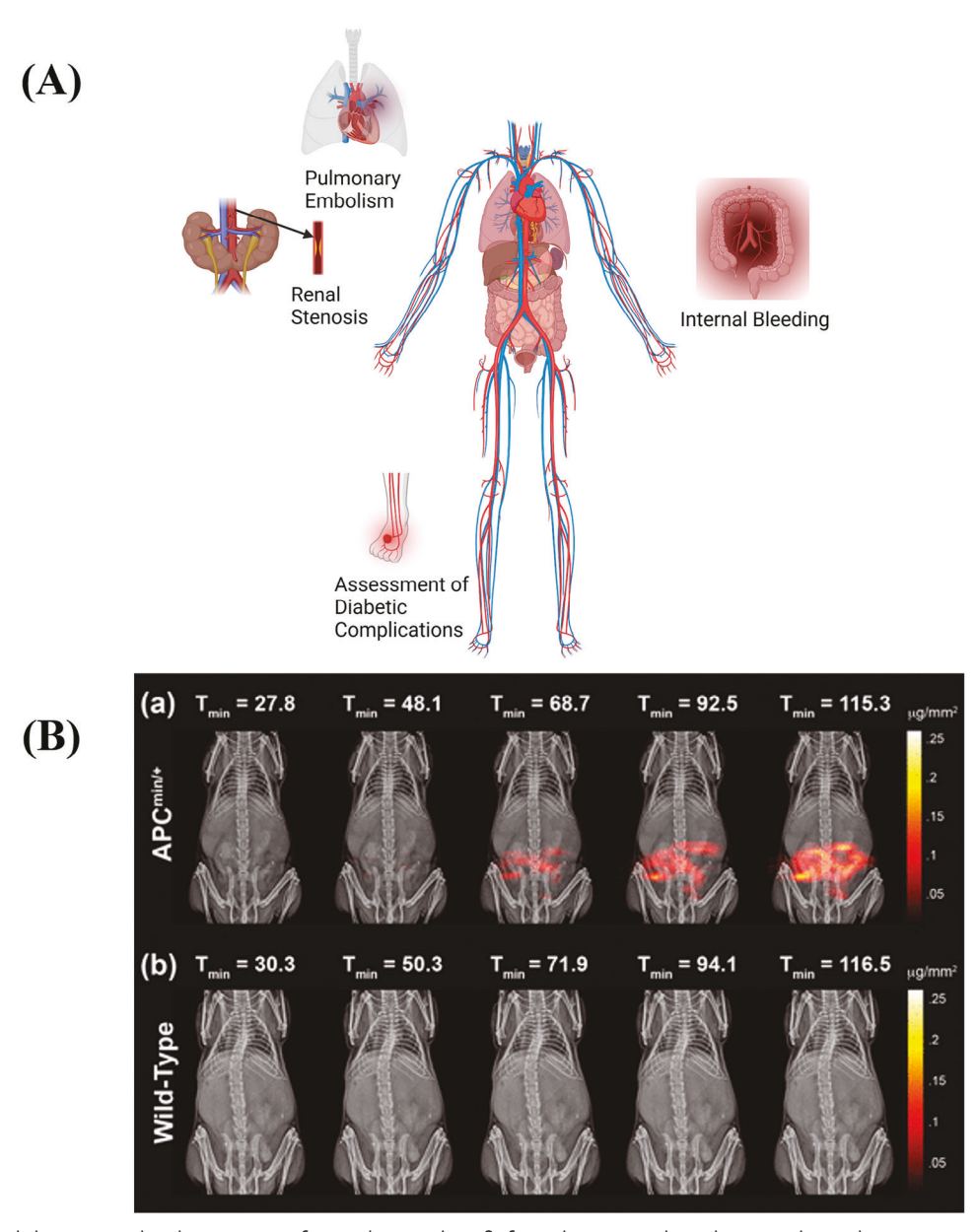


Figure 5. A) Clinical diagnoses related to organ perfusion that can benefit from the temporal resolution and signal generation of magnetic particle imaging (MPI). Limited background signal can improve detection and location of internal bleeding. Organ hemorrhage or stenosis can be detected and potentially quantified. B) An example of how MPI can be used to detect and quantify the rate of hemorrhage caused by a gut bleed by injecting the tracer LS-017 following induction of bleeding. Figure 5B is reproduced with permission. [87] Copyright 2020, American Chemical Society.

the kidney were visible in all groups. However, the number of vessels captured using both tracers in MPI was lower than that captured by MRA.

In a separate study, MPI was used to detect internal bleeding as opposed to organ perfusion (Figure 5B).[87] The tracer LS-017 was used with a custom scanner. A murine model that is predisposed to develop GI polyps (ApcMin/+) was given heparin to induce bleeding at the same time as the tracer was administered intravenously. The bleed was discerned and quantified by subtracting the initial time point image to account for circulating tracer. The circulation half-life determined by dynamic MPI signal decreased from ≈140 to ≈113 min in the disease group, indicating clearance through active bleeding. The bleeding rates were quantified to be between $\approx 2-4 \mu L \text{ min}^{-1}$. In a separate study, Mohn and colleagues demonstrated that they could detect leakage from the intestinal wall ex vivo and in a 3D printed bowel phantom.^[85] Additionally through the use of multiple tracers, they demonstrated that oral delivery of a tracer combined with intravenous delivery of a different tracer can enable multicontrast MPI with anatomical reference. This work is the first to demonstrate the potential, feasibility, and advancement in diagnostics achievable with MPI for intestinal wall ruptures, blockages, or leaks. Beyond this work, there has not been substantial application of MPI to monitor or detect internal bleeding from other commonly

www.advancedsciencenews.com

www.advhealthmat.de

21925259, 0, Downloaded from https://onlinelibrary.wiley.com/doi/10.1002adm.m.202400612 by University Of Flordat, Wiley Online Library for rules of use; OA articles are governed by the applicable Creative Commons Licensens and Conditions (https://onlinelibrary.wiley.com/remrs-and-conditions) on Wiley Online Library for rules of use; OA articles are governed by the applicable Creative Commons Licensens and Conditions (https://onlinelibrary.wiley.com/remrs-and-conditions) on Wiley Online Library for rules of use; OA articles are governed by the applicable Creative Commons Licensens and Conditions (https://onlinelibrary.wiley.com/remrs-and-conditions) on Wiley Online Library for rules of use; OA articles are governed by the applicable Creative Commons Licensens and Conditions (https://onlinelibrary.wiley.com/remrs-and-conditions) on Wiley Online Library for rules of use; OA articles are governed by the applicable Creative Commons Licensens and Conditions (https://onlinelibrary.wiley.com/remrs-and-conditions) on Wiley Online Library for rules of use; OA articles are governed by the applicable Creative Commons Licensens and Conditions (https://onlinelibrary.wiley.com/remrs-and-conditions) on Wiley Online Library for rules of use; OA articles are governed by the applicable Creative Commons Licensens and Conditions (https://onlinelibrary.wiley.com/remrs-and-conditions) on the conditions are governed by the applicable Creative Commons and Conditions are governed by the applicable Creative Commons and Conditions are governed by the applicable Creative Commons are governed by the applicable Creati

ADVANCED HEALTHCARE MATERIALS

injured organs (liver, spleen, etc.). In this context, longitudinal studies are needed to evaluate the effects of tracers outside of their typical clearance path to assess long-term safety.

The assessment of organ perfusion is also closely related to functional imaging, such as functional MRI (fMRI). In fMRI, brain activity is mapped based on increased blood flow and oxygen to regions of interest. fMRI depends on detection of water protons, which have a signal that is relatively weak and susceptible to physiological background. MPI has the potential to overcome these concerns by imaging a tracer that has been introduced directly to the blood stream. This directly visualizes the flow of the tracer in the blood with negligible background signal. The temporal resolution of MPI also makes it a great candidate as an improved functional imaging modality.

In one study, MPI was used to determine the cerebral blood volume in a hypercapnia rat model. [77] This study analyzed the potential of MPI as an alternative to fMRI. Using an unnamed PEGylated iron oxide tracer from Ocean Nanotech ($t_{1/2}$ estimated 1 h), the group found that when alternating between hyper/hypocapnia a signal difference of 10% was consistently observed. This suggests that MPI can detect differences in functional blood volume reliably. The difference in signal (\approx 10%) is larger than that typically reported in fMRI (\approx 1%).

In a 2023 report, the same group compared fMPI to fMRI directly with a similar hyper/hypocapnia cycle. [79] They found that the signal swing observed between cycles was 2–6× higher in the fMPI group than in the fMRI group. This finding highlights that fMPI can enable higher sensitivity functional imaging which, if combined with improved spatial resolution, could expand the impact of functional imaging by allowing patient-specific analysis, instead of relying on population averages. Initial studies have also demonstrated the feasibility of detecting tracer concentration differences in cerebral perfusion applications in nonhuman primates, [78] demonstrating clinical translation potential.

4. Future Perspectives and Goals for the Field

Based on the presented feasibility and characterization studies, MPI shows great potential as a diagnostic tool for imaging blood flow. Innovative imaging physics leads to advantageous characteristics such as improved penetration depth, temporal resolution, and limited signal attenuation during the imaging time course. Many other fields have also noted the promise of this technology, coupling imaging with other functional activities, such as inducing ferroptosis^[88] or targeted detection of specific antigens for quantitative imaging and assessments.^[1,89,90]

In this review, we focused on MPI research and feasibility studies aimed toward imaging blood circulation and pooling. While this review does not cover the substantial efforts toward optimizing SPION tracers^[91–93] and scanners for future human use,^[80,94–98] these contributions are crucial to the clinical implementation of MPI-based vascular imaging. Extensive work, not only synthesizing tailored tracers, but also in conducting comprehensive safety testing required for clinical use is nontrivial. Most of the research efforts reviewed within this manuscript used small animal scanners. However, as clinical-scale scanners are developed, maintaining spatial and temporal resolution poses challenges that must be addressed while ensuring sensitivity in SPION detection. For instance, achieving high spatial res-

Adv. Healthcare Mater. 2024, 2400612

olution necessitates large selection field gradients, thereby increasing power and cooling system requirements and the risk for peripheral nerve stimulation. In circulatory imaging specifically, temporal resolution is critical. As the field advances beyond the current preclinical scanners, selecting appropriate hardware and optimizing reconstruction algorithms becomes paramount. With advancements in data processing, deep learning, and artificial intelligence, the future of MPI-based imaging techniques holds significant promise. Researchers have investigated the application of deep learning concepts to enhance spatial resolution and mitigate edge effects in MPI images without the need for stronger magnetic gradients. Their efforts have yielded improved and reliable detection plaques and vessel branching in phantom models. [99,100] Other groups are working leveraging machine learning to enhance image restoration and segmentation. [101–103]

The work reviewed here concerning the optimization of tracers for blood pool imaging shows that there are limited tracers with high resolution and circulation half-lives longer than ≈30 min in mice (Figure 2). As more MPI tailored tracers become available, it will also be important to evaluate how the tracer properties impact the imaging at a desired site. Studies reviewed demonstrated how not only the tracer identity, but the local environment (e.g., viscosity^[81,61]) can modulate signal. It has been shown that imaging parameters are dependent upon the rates of flow and general transport at the site of assessment. This indicates that researchers should consider tracer identity for differing applications such as resolute small vessel assessments in the brain, compared to flow rates and volume differences in major vessels/chambers of the heart. As tracer design continues to move forward it is critical that the tracers are fully characterized not only in terms of their physical and colloidal properties, but also their magnetic properties. These properties should always be reported along with details of the scanner, reconstruction, and analysis set up used in application-based studies. This is important since users across different imaging setups and tracers can obtain confounding results.[104]

As the field moves forward, it is important that application studies focus on improving rigor and reproducibility. Many of the in vivo studies reviewed herein have one or two groups with a sample number between one and three. While this is sufficient to demonstrate feasibility, biological variability necessitates a higher sample number to demonstrate significance and reproducibility. On-going and future work should move toward studies demonstrating clear capabilities in clinical diagnostics. We see these efforts as multifold. First, preclinical and/or phantom studies need to focus on reproducibility and applicability for each potential clinical indication, identifying the appropriate timelines for tracer half-lives and optimized scanner settings, reconstruction, and analysis as a function of flow rates and expected noise. For example, a phantom and ex vivo study performed by Mohn et al. clearly outlines the conditions evaluated in the method section, using both a phantom model and ex vivo porcine bowel specimen.[85] However, the sample numbers are small and do not account for variability in patient populations (e.g., age) or comorbidities. Next, repeated small animal studies with optimized tracer and scanner settings for the given application should be done with higher sample numbers to enable rigorous statistical comparisons between MPI and existing imaging modalities, such as MRI. Once these two areas are fully addressed for

ADVANCED HEALTHCARE MATERIALS 21925259, 0, Downloaded from https://onlinelibrary.wiley.com/doi/10.1002adhm.202400612 by University Of Florata, Wiley Online Library on [01/07/2024]. See the Terms and Conditions (https://onlinelibrary.wiley.com/terms-and-conditions) on Wiley Online Library for rules of use; OA articles are governed by the applicable Creative Commons Licensens

specific clinical indications and as new larger-bore MPI scanners become available, large animal studies will need to focus on a better understanding of circulation half-lives, imaging at clinically relevant tissue depths, and the influence of blood flow rates, comparing how small animal models and expansive phantom or ex vivo data relate or even speak to scale-up toward expected humanlike conditions. It is well known that transport and fluid dynamics in large animal models vary greatly from small animal models. Validating phantom and ex vivo experiments against large animal studies will be critical for final translation to human patients.

It is also critical to consider how design and optimization of both tracers and MPI scanners can lead to use in other clinical indications. For example, two clinical scenarios that are likely to benefit from MPI technology are imaging of the small intestine and applications in diagnosis and evaluation or ovarian and uterine disease, such as endometriosis or cyst development. However, the fundamental investigations and use of animal models are substantially different between these two clinical indications. For example, evaluation of intestinal disease or injury in a mouse model is possible as many validated rodent injury and disease models exist across age groups.[105-107] Thus, it stands to reason that investigators could directly compare MPI to other imaging modalities such as MRI^[108,109] or CT imaging^[110] in a robust study design that looks to optimize MPI tracers and other key analysis parameters. Such rigorous small animal studies can allow for optimization studies along with initial safety and efficacy evaluations. Nevertheless, larger animal models representing intestinal disease or injury would still be needed to effectively demonstrate diagnostic relevance, such as the increase in resolution afforded by MPI, since large animal models enable more clinically relevant evaluation of penetration depth, diffusion, and circulation half-life. However, for many applications in women's health such as endometriosis, validated mouse models that recapitulate features and pathology of the disease in humans have been challenging to generate.^[111] Thus, for these applications, phantoms, ex vivo tissue analyses, and large animal studies will be necessary. We see a great potential for application of MPI in companion animals with similar challenges, such as those seen in canine ovarian cyst development,[112] canine or feline cystic endometrial hyperplasia, [113,114] or equine endometriosis [115] as a way to demonstrate future human feasibility and provide avenues for tracer optimization and scanner development and validation. These companion animal studies would pave the way toward MPI protocols for human clinical applications. To achieve these goals, human scale or large-scale scanners are required. These largerbore scanners are under development, [95] but increased access for the scientific and veterinary communities will be necessary to advance these technologies and realize their diagnostic potential.

Furthermore, as with any new technology or product, it is also important to consider what diagnostic applications are best left to existing imaging modalities and where MPI can offer substantial improvements over current standards of care. The cost of diagnostic imaging in clinics is nontrivial and access is not uniform, [116] so expectation of initial broad adoption outside of a research hospital may be challenging. Thus, as MPI moves toward clinical translation, it is important for studies to clearly demonstrate a significant advantage or unique diagnostic perspective that is not otherwise achieved with existing imaging modalities for applications of interest. An excellent example of

this is in the growing work on fMPI. The 10-fold improvement in signal difference in fMPI compared to signal differences reported in fMRI^[77] demonstrates potential for expanding the capabilities of functional imaging.^[79] Work to improve spatial resolution of functional MPI to fMRI levels is still necessary, but the demonstrated advantage in sensitivity covers a distinct gap in the capabilities of existing functional imaging techniques. In other studies, the MPI groups were outperformed by MRI in certain situations. As optimization continues this very well may change; however, continued consideration of what indications may benefit most from the use of MPI and how MPI would be utilized in a clinical setting alongside other available modalities is important to consider.

5. Outlook

Since the first report of MPI in 2005, [39] there have been impressive strides in demonstrating the potential of the technology using a wide range of techniques and strategies.[1] Part of this effort has focused on the development and validation of new tracers,[41,44,52,56] as different specifications may be required for specific clinical applications. However, as with the development of any new technology, strategies to standardize the methods used to assess new tracers and their application in various clinical settings will expand the field and improve the rate toward clinical manifestation. This review highlights several studies demonstrating the feasibility of MPI in the quantitative observation of blood circulation and pooling. As the field moves forward, it is important that future studies focus on robust confirmation of diagnostic related questions as well as comparison to existing imaging modalities to understand the differences in resulting data and diagnostic potential, but to also understand the differences in patient safety and risk. To fully answer these questions, collaboration between specialty clinicians (e.g., cardiologists), radiologists, and diagnosticians and materials scientists and engineers working to develop these technologies is paramount. Should future rigorous assessments demonstrate improved penetration depth and resolution as suggested by current feasibility studies, MPIbased imaging of blood circulation may revolutionize how we diagnose patients with injuries, perforations, or bleeding in clinical settings. The greatest potential is in the application of noninvasive MPI techniques to the diagnosis of injuries or diseases that usually require invasive procedures or laparoscopic surgery, such perforations of the small intestine or invasive endometriosis. Additionally, the imaging physics that enable direct signal generation and high temporal resolution can translate to improved functional imaging through MPI. This could support existing fMRI techniques in the transition of functional imaging from a neuroscience tool focused on trends to one of increased importance among diagnostics in individual patients.

Acknowledgements

Schematics in Figures 1, 3A, 4A, and 5A and the graphical abstract were created with a paid license from BioRender.com. The authors acknowledge the students enrolled in The University of Florida Chemical Engineering graduate class ECH 6937-Topics in Chemical Engineering I: Magnetic Nanoparticles in Spring 2023 for their insightful discussions and valuable feedback during peer reviews that led to this review paper. M.O.P. acknowledges support from the National Science Foundation Graduate Research

HEALTHCARE

2192259, 0, Downloaded from https://onlinelibrary.wiley.com/doi/10.1002/adhm.20240612 by University Of Florida, Wiley Online Library on [01.072024]. See the Terms and Conditions (https://onlinelibrary.wiley.com/terms-and-conditions) on Wiley Online Library for rules of use; OA articles are governed by the applicable Creative Commons I

Fellowship (DGE-2236414). W.L.S. acknowledges support from the National Institutes of Health, through the National Institute for General Medical Sciences award R35GM147041. CRR acknowledges support from the National Institutes of Health, through National Institute for Biomedical Imaging and Bioengineering award R01EB031224, National Cancer Institute award R21CA263653, and National Institute for Neurological Disorders and Stroke award R21NS125089. Any opinions, findings, and conclusions or recommendations expressed in this material are those of the author(s) and do not necessarily reflect the views of the National Science Foundation or another funding agency. W.L.S., M.O.P., and I.K.G. acknowledge support from the William P and Tracy Cirioli University of Florida Term Professorship.

Conflict of Interest

C.R.R. is an inventor in filed patents and invention disclosures related to this work.

Keywords

angiography, blood pool imaging, functional MPI, magnetic nanoparticles, magnetic particle imaging, SPIONs

> Received: February 17, 2024 Revised: May 11, 2024 Published online:

- [1] M. J. Ko, H. Hong, H. Choi, H. Kang, D. H. Kim, Adv. NanoBiomed. Res. 2022, 2, 2200053.
- [2] N. Panagiotopoulos, R. L. Duschka, M. Ahlborg, G. Bringout, C. Debbeler, M. Graeser, C. Kaethner, K. Ludtke-Buzug, H. Medimagh, J. Stelzner, T. M. Buzug, J. Barkhausen, F. M. Vogt, J. Haegele, Int. J. Nanomed. 2015, 10, 3097.
- [3] N. Talebloo, M. Gudi, N. Robertson, P. Wang, J. Magn. Reson. Imaging 2020, 51, 1659.
- [4] S. Lee, H. Huang, M. Zelen, Stat. Methods Med. Res. 2004, 13, 443.
- [5] R. A. de Boer, W. C. Meijers, P. van der Meer, D. J. van Veldhuisen, Eur. J. Heart Failure 2019, 21, 1515.
- [6] D. J. Omeh, E. Shlofmitz, Angiography, in StatPearls [Internet], Stat-Pearls Publishing, Treasure Island, FL 2023.
- [7] L. C. Wu, Y. Zhang, G. Steinberg, H. Qu, S. Huang, M. Cheng, T. Bliss, F. Du, J. Rao, G. Song, L. Pisani, T. Doyle, S. Conolly, K. Krishnan, G. Grant, M. Wintermark, AJNR Am. J. Neuroradiol. 2019, 40, 206.
- [8] X. Han, Y. Li, W. Liu, X. Chen, Z. Song, X. Wang, Y. Deng, X. Tang, Z. Jiang, Diagnostics 2020, 10, 800.
- [9] Y. R. Manda, K. M. Baradhi, StatPearls [Internet], https://www.ncbi. nlm.nih.gov/books/NBK531461/ (accessed: June 2023).
- [10] M. G. Bourassa, Can. J. Cardiol. 2005, 21, 1011.
- [11] K. L. Falk, S. Schafer, M. A. Speidel, C. M. Strother, AJNR Am. J. Neuroradiol. 2021, 42, 214.
- [12] R. F. Felipe, H. Prpic, J. W. Arndt, E. E. van der Wall, E. K. Pauwels, Eur. J. Radiol. 1991, 12, 20.
- [13] R. M. Witteles, J. W. Knowles, M. Perez, W. M. Morris, C. M. Spettell, T. A. Brennan, P. A. Heidenreich, Am. Heart J. 2012, 163, 617.
- [14] C. A. Pickett, M. K. Cheezum, D. Kassop, T. C. Villines, E. A. Hulten, Eur. Heart J. Cardiovasc. Imaging 2015, 16, 848.
- [15] V. Bodar, K. Modi, in StatPearls [Internet], StatPearls Publishing, Treasure Island, FL 2024.
- [16] J. D. van Dijk, J. Nucl. Cardiol. 2019, 26, 1981.
- [17] T. Massardo, R. Jaimovich, H. Lavados, D. Gutierrez, J. C. Rodriguez, J. M. Saavedra, R. Alay, H. Gatica, Eur. J. Nucl. Med. Mol. Imaging 2007, 34, 1735.

- [18] O. Akinboboye, K. Nichols, Y. Wang, U. R. Dim, N. Reichek, J. Nucl. Cardiol. 2005, 12, 418.
- [19] K. Nichols, R. Saouaf, A. A. Ababneh, R. J. Barst, M. S. Rosenbaum, M. W. Groch, A. H. Shoyeb, S. R. Bergmann, J. Nucl. Cardiol. 2002,
- [20] W.-W. Wee-Stekly, C. C. Y. Kew, B. S. M. Chern, Gynecol. Minimally Invasive Therapy 2015, 4, 106.
- V. Nisenblat, P. M. Bossuyt, C. Farquhar, N. Johnson, M. L. Hull, Cochrane Database Syst. Rev. 2016, 2, CD009591.
- [22] E. Pascoal, J. M. Wessels, M. K. Aas-Eng, M. S. Abrao, G. Condous, D. Jurkovic, M. Espada, C. Exacoustos, S. Ferrero, S. Guerriero, G. Hudelist, M. Malzoni, S. Reid, S. Tang, C. Tomassetti, S. S. Singh, T. Van den Bosch, M. Leonardi, Off. J. Int. Soc. Ultrasound Obstet. Gynecol. 2022, 60, 309.
- [23] C. Allaire, M. A. Bedaiwy, P. J. Yong, CMAJ 2023, 195, E363.
- [24] L. H. S. Lau, J. J. Y. Sung, Dig. Endosc. 2021, 33, 83.
- [25] C. E. Floyd, R. J. Jaszczak, K. L. Greer, R. E. Coleman, J. Nucl. Med. 1986, 27, 1577.
- [26] N. S. C. angiography, Am. J. Cardiol. 2001, 87, 15A.
- [27] R. Drescher, AJR Am. J. Roentgenol. 2013, 201, 908.
- [28] I. Danad, P. G. Raijmakers, R. S. Driessen, J. Leipsic, R. Raju, C. Naoum, J. Knuuti, M. Maki, R. S. Underwood, J. K. Min, K. Elmore, W. J. Stuijfzand, N. van Royen, Tulevski II, A. G. Somsen, M. C. Huisman, A. A. van Lingen, M. W. Heymans, P. M. van de Ven, C. van Kuijk, A. A. Lammertsma, A. C. van Rossum, P. Knaapen, JAMA Cardiol. 2017, 2, 1100.
- [29] R. P. Lim, I. Koktzoglou, Radiol. Clin. North Am. 2015, 53, 457.
- [30] A. Hussain, W. Steenbergen, I. M. Vellekoop, J. Biophotonics 2018, 11, 201700013.
- [31] B. W. Carney, G. Khatri, Cardiovasc. Diagn. Ther. 2019, 9.
- [32] H. Wei, O. T. Bruns, M. G. Kaul, E. C. Hansen, M. Barch, A. Wisniowska, O. Chen, Y. Chen, N. Li, S. Okada, J. M. Cordero, M. Heine, C. T. Farrar, D. M. Montana, G. Adam, H. Ittrich, A. Jasanoff, P. Nielsen, M. G. Bawendi, Proc. Natl. Acad. Sci. U. S. A. 2017, 114, 2325.
- [33] B. H. Kim, N. Lee, H. Kim, K. An, Y. I. Park, Y. Choi, K. Shin, Y. Lee, S. G. Kwon, H. B. Na, J. G. Park, T. Y. Ahn, Y. W. Kim, W. K. Moon, S. H. Choi, T. Hyeon, J. Am. Chem. Soc. 2011, 133, 12624.
- [34] Y. H. So, W. Lee, E. A. Park, P. K. Kim, Korean J. Radiol. 2021, 22, 1708.
- [35] A. Antonelli, C. Sfara, S. Battistelli, B. Canonico, M. Arcangeletti, E. Manuali, S. Salamida, S. Papa, M. Magnani, PLoS One 2013, 8, e78542.
- [36] X. Yang, G. Shao, Y. Zhang, W. Wang, Y. Qi, S. Han, H. Li, Front. Physiol. 2022, 13, 898426.
- [37] S. Harvell-Smith, L. D. Tung, N. T. K. Thanh, Nanoscale 2022, 14,
- [38] Z. W. Tay, S. Savliwala, D. W. Hensley, K. L. B. Fung, C. Colson, B. D. Fellows, X. Zhou, Q. Huynh, Y. Lu, B. Zheng, P. Chandrasekharan, S. M. Rivera-Jimenez, C. M. Rinaldi-Ramos, S. M. Conolly, Small Methods 2021, 5, e2100796.
- [39] B. Gleich, J. Weizenecker, Nature 2005, 435, 1214.
- [40] J. Nowak-Jary, B. Machnicka, J. Nanobiotechnol. 2022, 20, 305.
- [41] P. Keselman, E. Y. Yu, X. Y. Zhou, P. W. Goodwill, P. Chandrasekharan, R. M. Ferguson, A. P. Khandhar, S. J. Kemp, K. M. Krishnan, B. Zheng, S. M. Conolly, Phys. Med. Biol. 2017, 62, 3440.
- [42] G. Schütz, J. Lohrke, J. Hütter, Magnetic Nanoparticles: Particle Science, Imaging Technology, and Clinical Applications, World Scientific, Singapore 2010, pp. 32-36.
- [43] T. Yoshida, K. Enpuku, F. Ludwig, J. Dieckhoff, T. Wawrzik, A. Lak, M. Schilling, editors, Characterization of Resovist Nanoparticles for Magnetic Particle Imaging. Magnetic Particle Imaging: A Novel SPIO Nanoparticle Imaging Technique, Springer, Berlin 2012.
- [44] S. Liu, A. Chiu-Lam, A. Rivera-Rodriguez, R. De-Groff, S. Savliwala, N. Sarna, C. M. Rinaldi-Ramos, Nanotheranostics 2021, 5, 348.

HEALTHCARE

- [45] P. Reimer, B. T. Ferucarbotran, Eur. Radiol. 2003, 13, 1266.
- [46] M. H. Schwenk, Pharmacotherapy 2010, 30, 70.
- [47] AMAG Pharmaceuticals, https://www.feraheme.com/pdfs/ Feraheme-Dosing-and-Administration-Card.pdf (accessed: January 2024).
- [48] Miltenyi Biotec GmbH, https://static.miltenyibiotec.com/asset/ 150655405641/document_uqhv031jfl2r1dvgghjdne2l2j?contentdisposition=inline.
- [49] M. R. A. Abdollah, T. J. Carter, C. Jones, T. L. Kalber, V. Rajkumar, B. Tolner, C. Gruettner, M. Zaw-Thin, J. Baguna Torres, M. Ellis, M. Robson, R. B. Pedley, P. Mulholland, R. TMdR, K. A. Chester, ACS Nano 2018, 12, 1156.
- [50] Imagionbiosystems, https://imagionbiosystems.com/wp-content/ uploads/2022/08/PrecisionMRX-Info-Sheet.pdf.
- [51] P. Ludewig, M. Graeser, N. D. Forkert, F. Thieben, J. Randez-Garbayo, J. Rieckhoff, K. Lessmann, F. Forger, P. Szwargulski, T. Magnus, T. Knopp, Wiley Interdiscip. Rev. Nanomed. Nanobiotechnol. 2022, 14, e1757.
- [52] C. Lu, L. Han, J. Wang, J. Wan, G. Song, J. Rao, Chem. Soc. Rev. 2021, 50, 8102.
- [53] J. Rahmer, A. Antonelli, C. Sfara, B. Tiemann, B. Gleich, M. Magnani, J. Weizenecker, J. Borgert, *Phys. Med. Biol.* 2013, 58, 3965.
- [54] A. Antonelli, C. Sfara, J. Rahmer, B. Gleich, J. Borgert, M. Magnani, Biomed. Tech. 2013, 58, 517.
- [55] A. P. Khandhar, P. Keselman, S. J. Kemp, R. M. Ferguson, P. W. Goodwill, S. M. Conolly, K. M. Krishnan, *Nanoscale* 2017, 9, 1299.
- [56] H. Kratz, A. Mohtashamdolatshahi, D. Eberbeck, O. Kosch, F. Wiekhorst, M. Taupitz, B. Hamm, N. Stolzenburg, J. Schnorr, Nanomaterials 2021, 11, 1532.
- [57] H. Nejadnik, P. Pandit, O. Lenkov, A. P. Lahiji, K. Yerneni, Mol. Imaging Biol. 2019, 21, 465.
- [58] K. P. Doyle, L. N. Quach, H. E. Arceuil, M. S. Buckwalter, *Neurosci. Lett.* 2015, 584, 236.
- [59] L. Sandiford, A. Phinikaridou, A. Protti, L. K. Meszaros, X. Cui, Y. Yan, G. Frodsham, P. A. Williamson, N. Gaddum, R. M. Botnar, P. J. Blower, M. A. Green, R. T. de Rosales, ACS Nano 2013, 7, 500.
- [60] P. Chandrasekharan, Z. W. Tay, X. Y. Zhou, E. Yu, R. Orendorff, D. Hensley, Q. Huynh, K. L. B. Fung, C. C. VanHook, P. Goodwill, B. Zheng, S. Conolly, Br. J. Radiol. 2018, 91, 20180326.
- [61] K. Murase, R. X. Song, S. Hiratsuka, Appl. Phys. Lett. 2014, 104, 252409.
- [62] M. G. Kaul, J. Salamon, T. Knopp, H. Ittrich, G. Adam, H. Weller, C. Jung, Phys. Med. Biol. 2018, 63, 64001.
- [63] S. Herz, P. Vogel, T. Kampf, M. A. Ruckert, S. Veldhoen, V. C. Behr, T. A. Bley, *IEEE Trans. Med. Imaging* 2018, 37, 61.
- [64] P. Vogel, M. A. Ruckert, T. Kampf, S. Herz, A. Stang, L. Wockel, T. A. Bley, S. Dutz, V. C. Behr, IEEE Trans. Med. Imaging 2020, 39, 2133.
- [65] J. Franke, N. Baxan, H. Lehr, U. Heinen, S. Reinartz, J. Schnorr, M. Heidenreich, F. Kiessling, V. Schulz, *IEEE Trans. Med. Imaging* 2020, 39, 4335.
- [66] R. Siepmann, H. Nilius, F. Mueller, K. Mueller, C. Luisi, S. M. Dadfar, M. Straub, V. Schulz, S. D. Reinartz, PLoS One 2021, 16, e0249697.
- [67] J. Salamon, M. Hofmann, C. Jung, M. G. Kaul, F. Werner, K. Them, R. Reimer, P. Nielsen, A. Vom Scheidt, G. Adam, T. Knopp, H. Ittrich, PLoS One 2016, 11, e0156899.
- [68] S. Vaalma, J. Rahmer, N. Panagiotopoulos, R. L. Duschka, J. Borgert, J. Barkhausen, F. M. Vogt, J. Haegele, PLoS One 2017, 12, e0168902.
- [69] I. Molwitz, H. Ittrich, T. Knopp, T. Mummert, J. Salamon, C. Jung, G. Adam, M. G. Kaul, *Physiol. Meas.* 2019, 40, 105002.
- [70] J. Weizenecker, B. Gleich, J. Rahmer, H. Dahnke, J. Borgert, Phys. Med. Biol. 2009, 54, L1.
- [71] J. Sedlacik, A. Frolich, J. Spallek, N. D. Forkert, T. D. Faizy, F. Werner, T. Knopp, D. Krause, J. Fiehler, J. H. Buhk, *PLoS One* 2016, 11, e0160097.

- [72] W. Tong, H. Hui, W. Shang, Y. Zhang, F. Tian, Q. Ma, X. Yang, J. Tian, Y. Chen, *Theranostics* 2021, 11, 506.
- [73] W. Tong, Y. Zhang, H. Hui, X. Feng, B. Ning, T. Yu, W. Wang, Y. Shang, G. Zhang, S. Zhang, F. Tian, W. He, Y. Chen, J. Tian, EBioMedicine 2023, 90, 104509.
- [74] R. Orendorff, A. J. Peck, B. Zheng, S. N. Shirazi, R. Matthew Ferguson, A. P. Khandhar, S. J. Kemp, P. Goodwill, K. M. Krishnan, G. A. Brooks, D. Kaufer, S. Conolly, *Phys. Med. Biol.* 2017, 62, 3501.
- [75] P. Ludewig, N. Gdaniec, J. Sedlacik, N. D. Forkert, P. Szwargulski, M. Graeser, G. Adam, M. G. Kaul, K. M. Krishnan, R. M. Ferguson, A. P. Khandhar, P. Walczak, J. Fiehler, G. Thomalla, C. Gerloff, T. Knopp, T. Magnus, ACS Nano 2017, 11, 10480.
- [76] M. Graeser, F. Thieben, P. Szwargulski, F. Werner, N. Gdaniec, M. Boberg, F. Griese, M. Moddel, P. Ludewig, D. van de Ven, O. M. Weber, O. Woywode, B. Gleich, T. Knopp, *Nat. Commun.* 2019, 10, 1936.
- [77] C. Z. Cooley, J. B. Mandeville, E. E. Mason, E. T. Mandeville, L. L. Wald, NeuroImage 2018, 178, 713.
- [78] H. Hui, J. J. Liu, H. Zhang, J. Zhong, J. He, B. Zhang, H. R. Zhang, Q. Li, H. J. Li, J. Tian, IEEE Magn. Lett. 2023, 14, 11.
- [79] E. E. Mason, E. Mattingly, K. Herb, S. F. Cauley, M. Sliwiak, J. M. Drago, M. Graeser, E. T. Mandeville, J. B. Mandeville, L. L. Wald, Phys. Med. Biol. 2023, 68, 175032.
- [80] E. E. Mason, C. Z. Cooley, S. F. Cauley, M. A. Griswold, S. M. Conolly, L. L. Wald, Int. J. Magn. Part Imaging 2017, 3, 1703008.
- [81] P. Szwargulski, M. Wilmes, E. Javidi, F. Thieben, M. Graeser, M. Koch, C. Gruettner, G. Adam, C. Gerloff, T. Magnus, T. Knopp, P. Ludewig, ACS Nano 2020, 14, 13913.
- [82] M. G. Kaul, T. Mummert, C. Jung, J. Salamon, A. P. Khandhar, R. M. Ferguson, S. J. Kemp, H. Ittrich, K. M. Krishnan, G. Adam, T. Knopp, Phys. Med. Biol. 2017, 62, 3454.
- [83] X. Y. Zhou, K. E. Jeffris, E. Y. Yu, B. Zheng, P. W. Goodwill, P. Nahid, S. M. Conolly, Phys. Med. Biol. 2017, 62, 3510.
- [84] M. G. Kaul, T. Mummert, M. Graeser, J. Salamon, C. Jung, E. Tahir, H. Ittrich, G. Adam, Sci. Rep. 2021, 11, 4848.
- [85] F. Mohn, P. Szwargulski, M. G. Kaul, M. Graeser, T. Mummert, K. M. Krishnan, T. Knopp, G. Adam, J. Salamon, C. Riedel, Sci. Rep. 2023, 13, 22976.
- [86] X. Feng, P. Gao, Y. Li, H. Hui, J. Jiang, F. Xie, J. Tian, Bioeng. Transl. Med. 2024, 9, e10626.
- [87] E. Y. Yu, P. Chandrasekharan, R. Berzon, Z. W. Tay, X. Y. Zhou, A. P. Khandhar, R. M. Ferguson, S. J. Kemp, B. Zheng, P. W. Goodwill, M. F. Wendland, K. M. Krishnan, S. Behr, J. Carter, S. M. Conolly, ACS Nano 2017, 11, 12067.
- [88] M. J. Ko, S. Min, H. Hong, W. Yoo, J. Joo, Y. S. Zhang, H. Kang, D. H. Kim, *Bioact. Mater.* 2024, 32, 66.
- [89] W. Yang, Y. Wang, C. Fu, C. Li, F. Feng, H. Li, L. Tan, H. Qu, H. Hui, J. Wang, J. Tian, L. Long, *Theranostics* 2024, 14, 1081.
- [90] P. Gao, Y. Liu, X. Wang, X. Feng, H. Liu, S. Liu, X. Huang, X. Wu, F. Xiong, X. Jia, H. Hui, J. Jiang, J. Tian, Eur. J. Nucl. Med. Mol. Imaging 2024, 51, 1233.
- [91] A. P. Khandhar, R. M. Ferguson, H. Arami, S. J. Kemp, K. M. Krishnan, IEEE Trans. Magn. 2015, 51, 5300304.
- [92] X. Xie, J. Zhai, X. Zhou, Z. Guo, P. C. Lo, G. Zhu, K. W. Y. Chan, M. Yang, Adv. Mater. 2024, 36, 2306450.
- [93] L. M. Slavu, A. Antonelli, E. S. Scarpa, P. Abdalla, C. Wilhelm, N. Silvestri, T. Pellegrino, K. Scheffler, M. Magnani, R. Rinaldi, R. Di Corato, *Biomater. Sci.* 2023, 11, 3252.
- [94] E. Mattingly, M. Śliwiak, J. Drago, E. Mason, M. Graeser, L. Wald, Int. J. Magn. Part Imaging 2022, 8, 2203073.
- [95] E. Mattingly, E. Mason, M. Sliwiak, L. L. Wald, Int. J. Magn. Part Imaging 2022, 8, 2203075.
- [96] E. Mattingly, E. Mason, K. Herb, M. Śliwiak, J. Drago, M. Graeser, L. Wald, Int. J. Magn. Part Imaging 2022, 8, 212001.



www.advancedsciencenews.com

www.advhealthmat.de



21922659, 0, Downloaded from https://onlinelibrary.wiley.com/doi/10.1002/adhm.202400612 by University Of Florida, Wiley Online Library on [01/07/2024]. See the Terms

and Conditions

and-conditions) on Wiley Online Library for rules of use; OA articles are governed by the applicable Creative Commons I

- [97] L. L. Wald, Advances in Motion, https://advances.massgeneral.org/ radiology/article.aspx?id=1555 (accessed: January 2024).
- [98] P. Vogel, M. A. Ruckert, C. Greiner, J. Gunther, T. Reichl, T. Kampf, T. A. Bley, V. C. Behr, S. Herz, Sci. Rep. 2023, 13, 10472.
- [99] Y. Shang, J. Liu, L. Zhang, X. Wu, P. Zhang, L. Yin, H. Hui, J. Tian, Phys. Med. Biol. 2022, 67, 25012.
- [100] Y. Shang, J. Liu, Y. Liu, B. Zhang, X. Wu, L. Zhang, W. Tong, H. Hui, J. Tian, *Phys. Med. Biol.* **2023**, *68*, 45014.
- [101] S. Nigam, E. Gjelaj, R. Wang, G. W. Wei, P. Wang, J. Magn. Reson. Imaging 2024.
- [102] H. Hayat, A. Sun, H. Hayat, S. Liu, N. Talebloo, C. Pinger, J. O. Bishop, M. Gudi, B. F. Dwan, X. Ma, Y. Zhao, A. Moore, P. Wang, Mol. Imaging. Biol. 2021, 23, 18.
- [103] L. Wang, Y. Huang, Y. Zhao, J. Tian, L. Zhang, Y. Du, Mol. Imaging. Biol. 2023, 25, 788.
- [104] H. J. Good, O. C. Sehl, J. J. Gevaert, B. Yu, M. A. Berih, S. A. Montero, C. M. Rinaldi-Ramos, P. J. Foster, bioRxiv. 2023:2023.04.03.535446, https://doi.org/10.1101/2023.04.03.535446.
- [105] P. V. Gordon, A. C. Herman, M. Marcinkiewicz, B. M. Gaston, V. E. Laubach, J. L. Aschner, J. Pediatr. Gastroenterol. Nutr. 2007, 45, 509.
- [106] E. Mizoguchi, D. Low, Y. Ezaki, T. Okada, Intest. Res. 2020, 18, 151.
- [107] C. H. Lee, S. J. Koh, Z. A. Radi, A. Habtezion, *Intest. Res.* 2023, 21, 295

- [108] S. Bickelhaupt, M. C. Wurnig, M. Lesurtel, M. A. Patak, A. Boss, Lab. Anim. 2015, 49, 57.
- [109] D. Mustafi, X. Fan, U. Dougherty, M. Bissonnette, G. S. Karczmar, A. Oto, J. Hart, E. Markiewicz, M. Zamora, Magn. Reson. Med. 2010, 63, 922.
- [110] P. C. Naha, J. C. Hsu, J. Kim, S. Shah, M. Bouche, S. Si-Mohamed, D. N. Rosario-Berrios, P. Douek, M. Hajfathalian, P. Yasini, S. Singh, M. A. Rosen, M. A. Morgan, D. P. Cormode, ACS Nano 2020, 14, 10187.
- [111] K. A. Burns, A. M. Pearson, J. L. Slack, E. D. Por, A. N. Scribner, N. A. Eti, R. O. Burney, Front. Physiol. 2021, 12, 806574.
- [112] J. K. Sasidharan, M. K. Patra, L. K. Singh, A. C. Saxena, U. K. De, V. Singh, K. Mathesh, H. Kumar, N. Krishnaswamy, Top. Companion Anim. Med. 2021, 43, 100511.
- [113] D. H. Schlafer, A. T. Gifford, Theriogenology 2008, 70, 349.
- [114] M. Quartuccio, L. Liotta, S. Cristarella, G. Lanteri, A. Ieni, T. D'Arrigo, M. De Majo, Animals 2020, 10, 1368.
- [115] S. Schoniger, H. A. Schoon, Animals. 2020, 10, 625.
- [116] A. Phelan, J. Broughan, G. McCombe, C. Collins, R. Fawsitt, M. O'Callaghan, D. Quinlan, F. Stanley, W. Cullen, *PLoS One* 2023, 18, e0281461.





Marisa Pacheco is a Ph.D. candidate at the University of Florida in Chemical Engineering. She obtained her bachelor's degree in Chemical and Biological Engineering from the University of Colorado Boulder. Her current research focuses on the role of crystalline domains across silk fibroin based biomaterials.



Isabelle Gerzenshtein is an undergraduate student at the University of Florida, double majoring in Microbiology and Neuroscience, and pursuing a certificate in Artificial Intelligence. She is currently a research assistant under Marisa Pacheco and Dr. Whitney Stoppel.



Whitney Stoppel is an Assistant Professor in the Department of Chemical Engineering at the University of Florida. Prior to starting her faculty position, she obtained her Ph.D. in Chemical Engineering from the University of Massachusetts Amherst in 2014 and completed a postdoctoral fellowship in Biomedical Engineering at Tufts University from 2014–2018. Her research is motivated by a interest in understanding how nature builds materials and the use of these fundamental insights for the design and development of biomaterials for cardiovascular and musculoskeletal applications. Her group is particularly interested in silk fibroin biopolymers and the insects that produce them.



Carlos M. Rinaldi-Ramos is a Professor in the Department of Chemical Engineering and in the J. Crayton Pruitt Family Department of Chemical Engineering. His research interests span theory and simulation of magnetic nanoparticle response to dynamic magnetic fields, nanoparticle synthesis and surface modification, characterization of nanoparticle interactions with biological environments, and biomedical applications of magnetic nanoparticles including magnetic hyperthermia and magnetic particle imaging (MPI).